Plasma Neurofilament light and brain volumetric outcomes among middle-aged urban adults

Beydoun et. al.

ONLINE SUPPLEMENTARY MATERIAL

Online Supplemental Method 1. Brain structural/volumetric (s) magnetic resonance imaging (MRI) detailed description:

HANDLS description

sMRI

In addition to standard axial T1, T2, FLAIR images, high-resolution axial T1-weighted MPRAGE (TE = 2.32 ms, TR = 1900ms, TI = 900ms, flip angle = 9º, resolution = 256 × 256 × 96, FOV = 230 mm, sl. Thick. = 0.9 mm) of the brain was obtained for structural imaging. We used images as anatomic references and for the extraction of parameters of regional and whole brain volumes. T1-weighted MP-RAGE images covered the whole brain at a thickness of 1.2 mm for 160 sagittal slices (TR/TE/TI=2300/2.9/900 ms; FOV 25.6cm). These images were then converted to axial sections for comparative purposes.

The Section for Biomedical Image Analysis at the University of Pennsylvania developed techniques in-house to preprocess structural MRI scans. First, extra-cranial material on the T1-weighted images was removed using a multi-atlas registration method(Doshi et al., 2013). Bias was corrected using multiplicative intrinsic component optimization (MICO) method (Li et al., 2014). MUlti-atlas region Segmentation utilizing Ensembles (MUSE), segmented the pre-processed images into a set of anatomical regions of interest (ROIs) (Doshi et al., 2016). MUSE integrates a broad ensemble of labeled templates by using a number of warping algorithms, regularization atlases and parameters (Doshi et al., 2016).

Quality assurance

The Core for Translational Research in Imaging @ Maryland (C-TRIM), managed by the Department of Diagnostic Radiology at UMB's School of Medicine, has instituted several quality control measures to ensure highest level of quality and safety. The research-dedicated scanner undergoes routine quality data assurance as mandated by the American College of Radiology(Mulkern et al., 2008). In addition, the AD Neuroimaging Initiative phantom is used to assess weekly signal-to-noise ratio and monthly structural distortions(Gunter et al., 2009). We periodically check the reliability of diffusion data by utilizing the National Institutes of Standards and Technology diffusion phantom in order to ensure that the measurements from diffusion MRI are stable(phantom)

Online Supplemental Method 2: Plasma NfL sampling methodology

Plasma NfL was quantified in a sub-cohort of participants from HANDLS from visits v_1 (2004-2009), v_2 (2009-2013) and v_3 (2013-2018), from which we extracted data from only v_1 and v_2 for our present study. This sub-sample included participants from the HANDLS SCAN, an ancillary neuroimaging sub-study, (n=238)(Waldstein et al., 2017) This sub-study of the HANDLS cohort excluded participants with a history of dementia, stroke, transient ischemic attack, and carotid endarterectomy, MRI contraindications, terminal illness, HIV positivity or other neurological disorders (Waldstein et al., 2017). All HANDLS SCAN participants included in this sub-study had donated plasma samples at three different visits except for one participant that had samples from only 2 of 3 visits. In addition, we also included participants (n=463; 1389 samples) that donated plasma samples at v_1, v_2 and v_3, who were HIV negative, had complete cognitive tests [Trailmaking test, part A (TRAILS A) and Digits Span-Forward (DS-F)[at v_1 and v_2, Centers of Epidemiologic Studies-Depression (CES-D) scores at all 3 visits and with no history of HIV, stroke, transient ischemic attack, dementia, epilepsy, Parkinson's disease or brain cancer. Participants (n=3) were also included who had plasma samples available from v_1, v_2 and v_3, who also had genome wide DNA methylation data at v_1(Beydoun et al., 2019a; Beydoun et al., 2020; Tajuddin et al., 2019). These participants had the exclusions listed above. Thus, overall, N=694 HANDLS participants had plasma NfL data at v_1 ; N=709 at v_2 and N=707.

Online Supplemental Method 3: Mixed-effects linear regression models and empirical Bayes estimation

The main multiple mixed-effects regression models can be summarized as follows:

	Multi-level models vs. **Composite models**		
Eq.			
1.1-1.4	$Y_{ij} = \pi_{0i} + \pi_{1i} Time_{ij} + \varepsilon_{ij}$	$\pi_{0i} = \gamma_{00} + \gamma_{0a} X_{aij} + \sum_{k=1}^{l} \gamma_{0k} Z_{ik} + \zeta_{0i}$ $\pi_{1i} = \gamma_{10} + \gamma_{1a} X_{aij} + \sum_{m=1}^{n} \gamma_{1m} Z_{im} + \zeta_{1i}$	$Y_{ij} = \gamma_{00} + \gamma_{0a} X_{aij} + \sum_{k=1}^{l} \gamma_{0k} Z_{ik}$ $+ \gamma_{10} Time_{ij} + \gamma_{1a} X_{aij} Time_{ij}$ $+ \sum_{m=1}^{n} \gamma_{1m} Z_{im} Time_{ij}$ $+ (\zeta_{0i} + \zeta_{1i} Time_{ij} + \varepsilon_{ij})$

Where Y_{ij} is the outcome (plasma NfL, Log_e transformed) for each individual "i" and visit "j"; π_{0i} is the level-1 intercept for individual i; π_{1i} is the level-1 slope for individual i; γ_{00} is the level-2 intercept of the random intercept π_{0i} ; γ_{10} is the level-2 intercept of the slope π_{1i} ; Z_{ik} is a vector of fixed covariates for each individual *i* that are used to predict level-1 intercepts and slopes and included baseline age (Age_{base}) among other covariates. $X_{ija,}$ represents the main predictor variables. In this case, all predictor variables were socio-demographic and used for prediction. ζ_{0i} and ζ_{1i} are level-2 disturbances; ε_{ij} is the within-person level-1 disturbance. Main effect of TIME (γ_{1a}) and interactions with socio-demographic factors (γ_{1a}) along with random effects ζ_{1i} were used to estimate each individual slope π_{1i}, also known as the empirical bayes estimator. The time interval model is described in details in this methodological paper.(Blackwell et al., 2006) Since time is measured as year elapsed since visit 1 up till visit 2, the interpretation of π_{1i} is the predicted individual-level annual rate of change in the outcome Y_{ij}, between visits 1 and 2. This empirical bayes estimator of slope was used to examine association between annual rates of change in NfL (Log_e transformed) vs. brain MRI markers. Below are the results of the mixed effects regression models for the plasma NfL exposure:

Table III.1. Mixed-effects linear regression model for plasma NfL (Log_e transformed) over time, with random intercept and slope and fixed effects for v1 age, sex, race, and poverty status interacted with TIME.

	NfL (n=729, k=1.9)
Intercept (γ_{00} ±SE)	+2.087789±0.0301934***
Time (γ_{10} ±SE)	+0.0367367±0.0069329***
Age(v_1) γ_{01}±SE	+0.0260676±0.0018511***
Age(v_1)×Time, γ_{11}±SE	+0.0005684±0.0004078
Sex (0=Female, 1=Male), γ_{02}±SE	+0.0944587±0.0334616**
Sex×Time, γ_{12}±SE	+0.0080145±0.007381
Race (0=Whites, 1=AA), γ_{03}±SE	-0.1836598±0.0333263***
Race×Time, γ_{13}±SE	+0.0075765±0.0074284
Poverty (0=Below, 1=Above), γ_{04}±SE	+0.0373991± 0.036728
Poverty×Time, γ_{14}±SE	0.0044728±0.0080016
Var (ζ_{0i})	+0.1672103±0.0124954
Var (ζ_{1i})	+0.0062101±0.0009051
Var (ε_{ij})	+0.0249631±0.007274

***p<0.001; **P<0.010; *p<0.05

The empirical bayes estimator for annual rate of change in NfL, Log_e transformed, can be summarized as follows:

$\gamma_{10} + \gamma_{11}\times$ Age + $\gamma_{12}\times$ Sex + $\gamma_{13}\times$ Race + $\gamma_{14}\times$ Poverty + ζ_{1i}

Figure III.1 Baseline (v1), follow-up(v2) and annual rates of change in NfL scatter plot

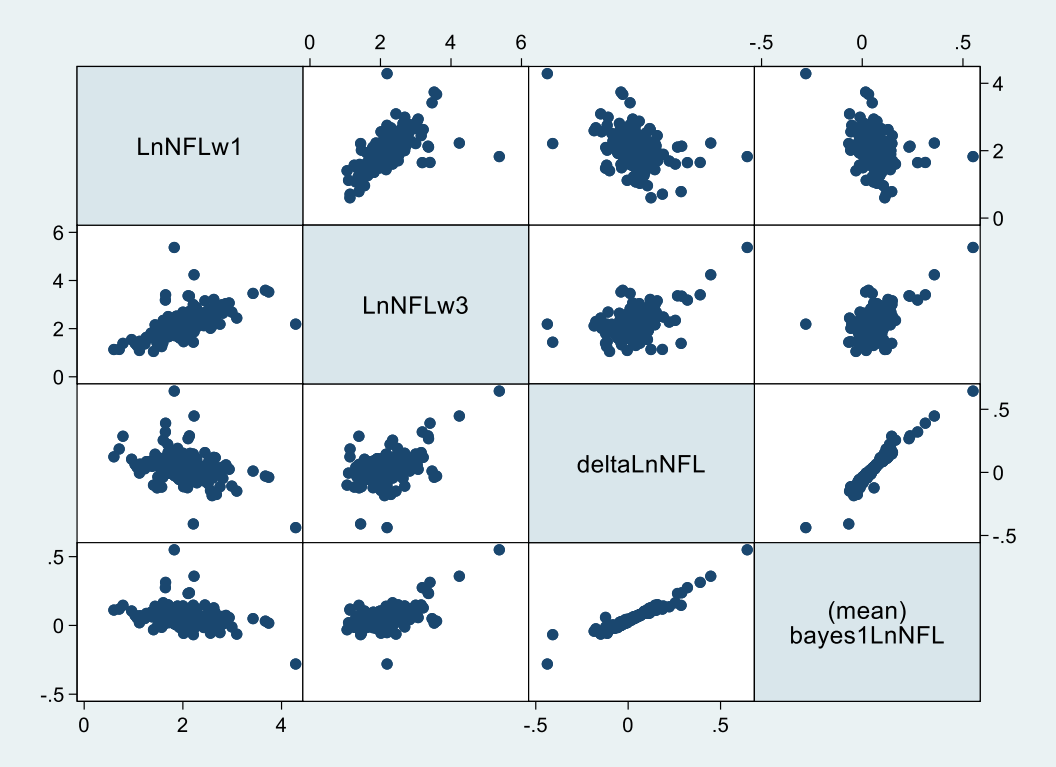

Abbreviations: NfL_{v1}=Plasma NfL (Log_e transformed) at visit 1 (HANDLS wave 1); NfLv2= Plasma NfL (Log_e transformed) at visit 2 (HANDLS wave 3); deltaNfL=Observed annual rate of change in Loge transformed NfL between visits 1 and 2; bayes1NfL=Empirical bayes estimator of annual rate of change in Loge transformed plasma NfL.

Supplemental Method 4: Additional covariates, LASSO regression and multiple imputations

A. Additional covariates:

A.1. Socio-demographic

Additional socio-demographic confounders included educational attainment (0 ≤ High School (HS); 1 = HS and 2 ≥ HS), the Wide Range Achievement Test (WRAT) letter and word reading subtotal scores to measure literacy, and marital status (1=married, 0=not married) (Beydoun et al., 2018).

A.2. Lifestyle

Smoking and drug use

Current use of opiates, marijuana or cocaine ("current" *vs*. "never or former") and smoking status ("current" vs. "never or former") were considered.

Adiposity measures

Measured body mass index (BMI, kg/m^2), waist circumference, and waist-hip-ratio were considered among potential confounders.

Healthy Eating Index 2010-

The Healthy Eating Index (HEI-2010) total score, based on two 24-hr recalls administered at baseline, was used as a measure of overall dietary quality. See steps for calculating HEI-2010 at http://appliedresearch.cancer.gov/tools/hei/tools.html and http://handls.nih.gov/06Coll-dataDoc.html.

Dietary Approaches to Stop Hypertension (DASH)

DASH diet adherence score, based on eight nutrients, was determined for each participant using the formula reported by Mellen *et al*.(Mellen et al.). The nine target nutrients were: total fat, saturated fat, protein, fiber, cholesterol, sodium, calcium, magnesium, and potassium. Micronutrient goals were expressed per 1000 kcal. The total DASH score was generated by the sum of all nutrient targets met. If the participant achieved the DASH target for a nutrient, a value of one was assigned, and if an intermediate target for a nutrient was achieved, a value of 0.5 was assigned. A value of zero was assigned if neither target was met. The maximum DASH score was nine; individuals meeting approximately half of the DASH targets (DASH score = 4.5) were considered DASH adherent (Mellen et al.).

Mean Adequacy Ratio (MAR)

Diet quality was also assessed using Nutrient Adequacy Ratio (NAR) and Mean Adequacy Ratio (MAR) scores(Fanelli Kuczmarski et al., 2013; Murphy et al., 2006). NAR score was determined by taking each participant's daily intake of a nutrient divided by the Recommended Dietary Allowance (RDA) for that nutrient. NAR scores were determined for 17 micronutrients: vitamins A, C, D, E, B_6, B_{12}, folate, iron, thiamin, riboflavin, niacin, copper, zinc, calcium, magnesium, phosphorus, and selenium. The RDA was adjusted for participants' ages and sexes and vitamin C was adjusted for smokers(Murakami et al., 2019). The NAR score was converted into a percent with values exceeding 100 truncated to 100. MAR scores were calculated by averaging the NAR scores: MAR= (∑NAR scores)/17(Fanelli Kuczmarski et al., 2018). NAR and MAR were calculated separately for each daily-intake and then averaged. MAR scores, based on food intakes only, were used as the nutrient-based diet quality variable.

Depressive symptoms

Depressive symptoms were operationalized using the CES-D at baseline and follow-up. The 20-item CES-D is a self-reported symptom rating scale assessing affective and depressed mood.(Radloff, 1977) A score of ≥16 on the CES-D is reflective of elevated depressive symptoms (EDS), (Ramos et al., 2004) and predicts clinical depression based on the Diagnostic and Statistical Manual, fourth edition (DSM-IV) criteria.(Myers and Weissman, 1980) Four CES-D sub-domains exhibiting an invariant factor structure between The National Health and Nutrition Examination Survey I and pilot HANDLS data (Nguyen et al., 2004) were computed. We tested our hypotheses using total and domain-specific CES-D scores: **(1)** Somatic complaints; **(2)** Depressive affect; **(3)** Positive affect and **(4)** Interpersonal problems.(Nguyen et al., 2004)

A.3. Health-related

Baseline chronic conditions included self-reported history measurement, biomarker-based measurement, and medication-based measurement, of type 2 diabetes, hypertension, dyslipidemia, cardiovascular disease, and inflammatory disease. Dyslipidemia was based on a combination of self-report, HDL, total cholesterol, triglyceride criteria, and statin use. Similarly, type 2 diabetes was determined using a combination of self-report, serum glucose criteria and medication. The same was conducted for hypertension. Additionally, a composite of cardiovascular

disease history was added in which self-reported stroke, congestive heart failure, non-fatal myocardial infarction or atrial fibrillation combined into a yes/no variable. Similarly, inflammatory disease was a binary composite of multiple sclerosis, systemic lupus, gout, rheumatoid arthritis, psoriasis, Thyroid disorder and Crohn's disease. The use of NSAIDs (prescription and over the counter) and statins over the past two weeks were considered separately as potential covariates.

A.4. Other biomarkers

All laboratory tests selected for this study were done at Quest Diagnostics, Chantilly, VA.

Serum cholesterol and atherogenic indices

Total cholesterol (TC), High density lipoprotein-cholesterol (HDL-C) and Triacylglycerols (TA) were assessed using a spectrophotometer (Olympus 5400). Low density lipoprotein-cholesterol (LDL-C) was calculated as TC-(HDL-C+TA/5) and directly measured in a sub-sample (N=236) using a spectrophotometer (Olympus 5400). The correlation between those with baseline calculated LDL-C and those with measured LDL-C was r~0.95. From these calculations, two relative measures were obtained, namely TC: HDL-C and LDL-C: HDL-C ratios. These were termed "atherogenic indices" and have been previously studied in relation to various cardiovascular outcomes that found them to be positively associated with measures of atherosclerosis and coronary heart disease. (Hisamatsu et al., 2014; Manickam et al., 2011; Nair et al., 2009)

Serum uric acid (SUA)

SUA measurements are useful in the diagnosis and treatment of renal and metabolic disorders, including renal failure, gout, leukemia, psoriasis, starvation or other wasting conditions, as well as in patients receiving cytotoxic drugs. Using 1 ml of fasting blood serum, uric acid was measured using a standard spectrophotometry method. The reference range for adult men is 4.0-8.0 mg/dL, whereas for women the range is 2.5-7.0 mg/dL. (http://www.questdiagnostics.com/testcenter/TestDetail.action?ntc=905) Other reference ranges were also recently suggested and depend on the menopausal status of women. Those reference ranges are based on predictive value for gout outcomes among healthy individuals and do not necessarily predict other pathologies. Thus, based on recent research evidence, a "normal" SUA value is suggested to be <6.0 mg/dL for all healthy adult individuals.

Serum albumin

Using 0.5-1 mL samples of plasma prepared with heparin and refrigerated for up to 30 days, albumin was measured with spectrophotometry, with an expected reference range of 3.6-5.1 g/dL(Beydoun et al., 2016b; Beydoun et al., 2019b).

High sensitivity C-reactive protein (CRP)

High sensitivity CRP (hs-CRP) was analyzed with an immunoturbidimeter (Siemens/Behring Nephelometer II), using 0.5-1 mL of plasma. A range of 1-10 mg/dL indicates average to high cardiovascular risk and >10 mg/dL suggests an infection or a chronic inflammation.

Serum creatinine

Using participant fasting blood specimens, baseline serum creatinine was measured at the National Institute on Aging, Clinical Research Branch Core Laboratory, using a modified kinetic Jaffe method (CREA method, Dade Dimension X-Pand Clinical Chemistry System, Siemens Healthcare Diagnostics Inc., Newark, DE) for a small group of participants (n=88). However, a majority of participants (n=1,528) had baseline serum creatinine analyzed at Quest Diagnostics, Inc. by isotope dilution mass spectrometry (IDMS) (Olympus America Inc., Melville, NY) and standardized to the reference laboratory, Cleveland Clinic. While inter-assay coefficients of variation (CV) for this sample could not be calculated due to the use of only one or the other measurement of creatinine at baseline, only intra-assay CVs (mean/SD) could be estimated. These were 0.192 and 0.187 for the CREA and the IDMS methods, respectively.

HbA1c

Glycated hemoglobin is derived from the nonenzymatic addition of glucose to amino groups of hemoglobin. HbA1c is a specific glycated hemoglobin that results from the attachment of glucose to the N-terminal valine of the hemoglobin b-chain. Numerous assays were subsequently developed to measure glycated hemoglobins. The principle of all methods is to separate the glycated and nonglycated forms of hemoglobin(Beydoun et al., 2016a). This can be accomplished based on differences in charge (usually by HPLC) or structure (usually immunoassays or boronate affinity chromatography). In this study, HPLC was used (Quest diagnostics).

White blood cell inflammatory markers

Fasting blood samples were collected from participants at baseline and follow-up to determine total white blood cell count (K/mm^3), using electronic Cell Sizing, counting, cytometry, and microscopy. (http://www.questdiagnostics.com/testcenter/TestDetail.action?ntc=7064).

Serum 25-hydroxyvitamin D, folate and cobalamin

Participants were asked to fast for ≥8 hours prior to the MRV visits, and serum specimens in volumes of 2 mL were collected and frozen at −80°C. Similar procedures were adopted for serum folate and cobalamin, both measured using chemiluminescence immunoassay (Siemens Centaur) by Quest Diagnostics, Chantilly, VA (Diagnostics; Wolters et al., 2005), and previously validated against other automated methods with coefficient of variation (CV) < 10% (Ispir et al., 2015; Owen and Roberts, 2003).

25(OH)D were measured using slightly revised methodologies between v_1 and v_2. In this study, only the v_1 measure was used. At v_1, total levels of serum 25(OH)D (in ng/ml; D_2 and D_3) were measured using tandem mass spectrometry (interassay CV, 8.6%) at Massachusetts General Hospital for less than 60 days later, as recommended for frozen samples (Powe et al., 2013). Blood samples drawn at examination were stored at −80°C.

Dietary and supplemental intakes of vitamin D, folate and cobalamin were shown to moderately correlate with their corresponding serum biomarkers in HANDLS and national surveys (Beydoun et al., 2010a; Beydoun et al., 2018; Beydoun et al., 2010b).

Hemoglobin and other hematological measures

Hemoglobin (Hb)

Similarly, using electronic cell sizing/cytometry/microscopy, Hb was assayed from a sample of 1 ml of blood drawn from participants after an overnight fast, and refrigerated up to 6 days (Quest diagnostics).

Other hematological markers

Ferritin: Ferritin is decreased in iron deficiency anemia and increases with iron overload. It is measured with immunoassay with reference ranges of 20-380 ng/mL among men and 10-232 ng/mL among women.(Diagnostics)

Erythrocyte Sedimentation Rate (ESR): Using 5 mL of refrigerated whole blood stored in lavender top EDTA tubes, the ESR was tested within 24 hr of blood draw. This test used automated modified Westergren photochemical capillary-stopped flow kinetic analysis.(Diagnostics; Larsson and Hansson, 2004) The Mayo Clinic reports a reference of 0-22 mm/hr for men and 0-29 mm/hr for women(Mayo Clinic, 2017) and is considered a proxy measure for serum fibrinogen.(Yin et al., 2017)

Serum iron: 0.5-1 mL of fasting serum was collected, transported at room temperature (with heparin added) and refrigerated or frozen subsequently. Serum iron was measured with spectrophotometry, (Diagnostics; Samarina and Proskurnin, 2015) with reference ranges for men aged ≥30y set at 50-180 µg/dL, and for women: 20-49y (40-190 µg /dL) and 50+y(45-160 µg /dL). (Diagnostics)

Mean Corpuscular Volume (MCV): Also known as erythrocyte mean corpuscular volume, MCV is measured using standard electronic cell sizing/counting/cytometry/microscopy. Similar to other hemogram measures (e.g. ESR), a microtainer 1 mL whole blood in an EDTA (lavender-top) tube was transported at room temperature to the laboratory facility.(Diagnostics)

Mean Cell Hemoglobin (MCH): The hematologic index MCH was calculated as follows: MCH = Hb/RBC.

Red Cell Distribution Width (RDW): RDW was calculated by automated Coulter DXH 800 hematology analyzer as part of peripheral complete blood count (Beckman Coulter, Brea, CA). The analyzer underwent regular calibration every three months and quality control procedures (Diagnostics). Clinical analysis typically includes two RDW measurements, i.e. the RDW-CV (unit: %), which we adopted in this study, and the RDW-Standard Deviation (SD, unit: fL) from which RDW-CV is obtained. RDW-CV=RDW-SD×100/MCV, MCV being the mean cell volume. RDW-CV's normal range is 11.0 - 15.0%, and it depends on width of the distribution (normal range: 40-55 fL) curve and MCV (techs, 2019).

Other measures and their methods of quantification are listed below:

Variable	HANDLS Variable Label	Description	Source
ALP	Alkaline phosphatase (U/L)	This liver enzyme was measured at Quest diagnostics using spectrophotometry. URL: https://testdirectory.questdiagnostics.com/test/test-detail/234/alkalinephosphatase?cc=MASTER	https://handls.nih.gov/pubs/2021-Beydoun-AffectiveDisorders-282-858.pdf
ALT	ALT [SGPT] (U/L)	Beckman Coulter AU5400®	https://www.ncbi.nlm.nih.gov/pmc/articles/PMC5882538/
Amylase	Amylase (U/L)	Spectrophotometry Reference Range(s) 21-101 U/L	https://testdirectory.questdiagnostics.com/test/test-detail/243/amylase?cc=MASTER
AST	AST [SGOT] (U/L)	Beckman Coulter AU5400®	https://www.ncbi.nlm.nih.gov/pmc/articles/PMC5882538/
BiliDir	Direct [conjugated] bilirubin (mg/dL)	Spectrophotometry	https://testdirectory.questdiagnostics.com/test/test-detail/287/bilirubin-total?cc=MASTER
BiliTot	Total bilirubin (mg/dL)	Spectrophotometry	https://testdirectory.questdiagnostics.com/test/test-detail/287/bilirubin-total?cc=MASTER
BUN	Blood urea nitrogen (mg/dL)	Beckman Coulter AU5400®	https://www.ncbi.nlm.nih.gov/pmc/articles/PMC5882538/
Calcium	Calcium (mg/dL)	Spectrophotometry	https://testdirectory.questdiagnostics.com/test/test-detail/303/calcium?cc=MASTER
Cl	Chloride (mmol/L)	Ion Selective Electrode (ISE) Reference Range(s) 98-110 mmol/L	https://testdirectory.questdiagnostics.com/test/test-detail/330/chloride?cc=MASTER

CO2	Carbon dioxide (mmol/L)	Spectrophotometry Reference Range(s) 20-32 mmol/L	https://testdirectory.questdiagnostics.com/test/test-detail/310/carbon-dioxide?cc=MASTER
EosinPct	WBC Eosinophil (%)	Electronic Counting and Sizing • Cytometry • Microscopy	https://testdirectory.questdiagnostics.com/test/test-detail/425/eosinophil-count-blood?cc=MASTER
FeSat	Iron saturation (%)	1.1.1 Spectrophotometry 1.1.2 1.1.3 Minimum Volume: 0.5 mL 1.1.4 Transport Temperature: Room temperature 1.1.5 Specimen Stability • Room temperature: 6 days • Refrigerated: 7 days • Frozen: 28 days	https://testdirectory.questdiagnostics.com/test/test-detail/7573/iron-total-and-total-iron-binding-capacity?cc=MASTER
GGT	Gamma glutamyl transferase (U/L)	Spectrophotometry 1.1.6 Preferred Specimen(s): 1 mL serum 1.1.7 Minimum Volume: 0.5 mL Specimen Stability • Room temperature: 7 days • Refrigerated: 7 days • Frozen: 28 days	https://testdirectory.questdiagnostics.com/test/test-detail/482/gamma-glutamyl-transferase-ggt?cc=MASTER
HBV	Hepatitis B surface antigen	Immunoassay (IA) 1.1.8 Minimum Volume: 1 mL 1.1.9 Transport Temperature: Room temperature 1.1.10 Specimen Stability • Room temperature: 7 days • Refrigerated: 14 days • Frozen: 30 days	https://testdirectory.questdiagnostics.com/test/test-detail/498/hepatitis-b-surface-antigen-with-reflex-confirmation?cc=MASTER
Hct	Hematocrit (%)	Electronic Cell, Sizing/Cytometry/Microscopy 1.1.11 Minimum Volume: Microtainer: 0.5 mL • EDTA (lavender-top) tube: 1 mL 1.1.12 1.1.13 Transport Temperature: Room temperature 1.1.14 1.1.15 Specimen Stability • Room temperature: 48 hours • Refrigerated: 48 hours (may cause platelet clumping) • Frozen: Unstable	https://testdirectory.questdiagnostics.com/test/test-detail/509/hematocrit?cc=MASTER

HCV	Hepatitis C	Immunoassay (IA) 1.1.16 Minimum Volume: 3 mL 1.1.17 Transport Temperature: Room temperature 1.1.18 Specimen Stability • Room temperature: 72 hours • Refrigerated: 14 days • Frozen: 30 days	https://testdirectory.questdiagnostics.com/test/test-detail/8472/hepatitis-c-antibody-with-reflex-to-hcv-rna-quantitative-real-time-pcr?cc=MASTER
Insulin	Serum insulin (uIU/mL)	Immunoassay (IA) 1.1.19 Reference Range(s) ≤19.6 uIU/mL 1.1.20 Minimum Volume: 0.5 mL 1.1.21 Transport Temperature: Refrigerated (cold packs) 1.1.22 Specimen Stability • Room temperature: 8 hours • Refrigerated: 7 days • Frozen: 28 days	https://testdirectory.questdiagnostics.com/test/test-detail/561/insulin?cc=MASTER
K	Potassium (mmol/L)	Beckman Coulter AU5400®	https://www.ncbi.nlm.nih.gov/pmc/articles/PMC5882538/
LDH	Lactate dehydrogenase (U/L)	Beckman Coulter AU5400®	https://www.ncbi.nlm.nih.gov/pmc/articles/PMC5882538/
MCH	Mean cell hemoglobin (pg)	The hematologic index MCH was calculated as follows: MCH = Hb/RBC.	
MCV	Mean cell volume (fL)	Reference range: 80.0 - 100.0 fL	https://www.radc.rush.edu/docs/var/detail.htm?category=Blood%20Measures&subcategory=Routine%20laboratory%20tests&variable=mcv
Mg	Magnesium (mg/dL)	Spectrophotometry 1.1.23 Reference Range(s): 1.5-2.5 mg/dL 1.1.24 Minimum Volume: 0.5 mL 1.1.25 Transport Temperature: Room temperature 1.1.26 1.1.27 Specimen Stability • Serum and plasma • Room temperature: 7 days • Refrigerated: 7 days • Frozen: 28 days	https://testdirectory.questdiagnostics.com/test/test-detail/622/magnesium?cc=MASTER

Na	Sodium (mmol/L)	Ion Selective Electrode (ISE) 1.1.28 Reference Range(s): 135-146 mmol/L 1.1.29 Minimum Volume: 0.5 mL 1.1.30 Transport Temperature: Room temperature	https://testdirectory.questdiagnostics.com/test/test-detail/836/sodium?cc=MASTER
Phosphate	Phosphate (mg/dL)	Spectrophotometry 1.1.31 Minimum Volume: 0.5 mL 1.1.32 Transport Temperature: Room temperature 1.1.33 Specimen Stability • Room temperature: 72 hours • Refrigerated: 7 days • Frozen: 28 days	https://testdirectory.questdiagnostics.com/test/test-detail/718/phosphate-as-phosphorus?cc=MASTER
Platelets	Platelet count (10^9/L)	Electronic Cell Sizing/Counting/Cytometry/Microscopy Reference Range(s) ≤3 Days 150-450 Thousand/µL 4 Days-6 Months 150-400 Thousand/µL >6 Months 140-400 Thousand/µL 1.1.34 Minimum Volume: Microtainer 0.5 mL 1 mL whole blood EDTA (lavender-top) tube 1.1.35 1.1.36 Transport Temperature: Room temperature - do not refrigerate 1.1.37 1.1.38 Specimen Stability • Room temperature: 48 hours • Refrigerated: Not provided • Frozen: Not provided	https://testdirectory.questdiagnostics.com/test/test-detail/723/platelet-count-edta?cc=MASTER
RPR	RPR screen	Flocculation 1.1.39 Reference Range(s): Non-Reactive 1.1.40 Preferred Specimen(s): 1 mL serum 1.1.41 1.1.42 Specimen Stability • Room temperature: 4 days • Refrigerated: 7 days • Frozen: 30 days	https://testdirectory.questdiagnostics.com/test/test-detail/799/rpr-monitor-with-reflex-to-titer?cc=MASTER

T3uptake	T3 uptake (%)	Immunoassay (IA) 1.1.43 Reference Range(s): 22-35 % 1.1.44 Minimum Volume: 0.5 mL 1.1.45 Transport Temperature: Room temperature 1.1.46 Specimen Stability • Room temperature: 7 days • Refrigerated: 10 days • Frozen: 28 days	https://testdirectory.questdiagnostics.com/test/test-detail/861/t3-uptake?cc=MASTER
T4Feee	T4 free n(g/dL)	Immunoassay (IA) 1.1.47 Minimum Volume: 0.3 mL 1.1.48 Transport Temperature: Room temperature 1.1.49 Specimen Stability • Room temperature: 7 days • Refrigerated: 7 days • Frozen: 28 days	https://testdirectory.questdiagnostics.com/test/test-detail/866/t4-free-ft4?cc=MASTER
T4tot	T4 [thyroxine] total mcg/dL	Immunoassay (IA) 1.1.50 Minimum Volume: 0.5 mL 1.1.51 Transport Temperature: Room temperature 1.1.52 Specimen Stability • Room temperature: 7 days • Refrigerated: 7 days • Frozen: 28 days	https://testdirectory.questdiagnostics.com/test/test-detail/867/t4-thyroxine-total?cc=MASTER
TIBC	Total iron binding capacity mcg/dL	Spectrophotometry 1.1.53 Minimum Volume: 0.5 mL 1.1.54 Transport Temperature: Room temperature 1.1.55 Specimen Stability • Room temperature: 6 days • Refrigerated: 7 days • Frozen: 28 days	https://testdirectory.questdiagnostics.com/test/test-detail/7573/iron-total-and-total-iron-binding-capacity?cc=MASTER
Triglyc	Triglyceride (mg/dL)	Spectrophotometry Reference Range(s): <150 mg/dL	https://testdirectory.questdiagnostics.com/test/test-detail/896/triglycerides?cc=MASTER

		1.1.56 Minimum Volume: 0.5 mL 1.1.57 Transport Temperature: Room temperature 1.1.58 Specimen Stability • Serum and plasma • Room temperature: 5 days • Refrigerated: 7 days • Frozen: 28 days	
TSH	Thyroid-stimulating hormone (mIU/L)	Immunoassay (IA) 1.1.59 Minimum Volume: 0.7 mL 1.1.60 Transport Temperature: Room temperature 1.1.61 Specimen Stability • Room temperature: 7 days • Refrigerated: 7 days • Frozen: 28 days	https://testdirectory.questdiagnostics.com/test/test-detail/899/tsh?cc=MASTER
UpH	Urine pH	pH Meter 1.1.62 Reference Range(s): 4.6-8.0 1.1.63 Minimum Volume: 10 mL 1.1.64 Transport Temperature: Room temperature	https://testdirectory.questdiagnostics.com/test/test-detail/8452/ph-urine?cc=MASTER
USpecGrav	Urine specific gravity	Reagent Impregnated Strips 1.1.65 Reference Range(s): 1.001-1.035 1.1.66 1.1.67 Minimum Volume: Preserved: 1 mL 1.1.68 Transport Temperature: Preserved: Room temperature 1.1.69	https://testdirectory.questdiagnostics.com/test/test-detail/3190/specific-gravity-urine?cc=MASTER
Eosinophils	WBC Eosinophil count (10^9/L)	Methodology Electronic Counting and Sizing • Cytometry • Microscopy	https://testdirectory.questdiagnostics.com/test/test-detail/425/eosinophil-count-blood?cc=MASTER
Lipase	Lipase (U/L)	Spectrophotometry; Reference Range(s) 7-60 U/L	https://testdirectory.questdiagnostics.com/test/test-detail/606/lipase?cc=MASTER
UCreatinine	Urine creatinine	Colorimetric (C) • Kinetic	https://testdirectory.questdiagnostics.com/test/test-detail/8459/creatinine-random-urine?cc=MASTER

		1.1.70 Preferred Specimen(s): 10 mL random urine, no preservative 1.1.71 Minimum Volume: 0.5 mL 1.1.72 Transport Temperature: Room temperature 1.1.73 Specimen Stability • Room temperature: 7 days • Refrigerated: 7 days • Frozen: 28 days	
UMicroAlb	Urine microalbumin	Immunoturbimetric assay (Kamiya Biomedical Co., Seattle, WA). CKD was defined as an estimated glomerular filtration rate (eGFR) <60 mL/min per 1.73 m2 calculated using the CKD Epidemiology Collaboration creatinine-based equation	immunoturbimetric assay (Kamiya Biomedical Co., Seattle, WA). CKD was defined as an estimated glomerular filtration rate (eGFR) <60 mL/min per 1.73 m2 calculated using the CKD Epidemiology Collaboration creatinine-based equation

B. Least absolute shrinkage and selection operator (LASSO) regression procedure

In order to select the appropriate set of predictive models for NfL, we used a statistical learning method for variable selection known as adaptive LASSO and compared it to cross-validation LASSO (cvLASSO) and lowest BIC LASSO. Socio-demographic variables, (age, sex, race/ethnicity, poverty status) were force entered as fixed terms into all models. The LASSO then selected among the other covariates listed above as variables that should be retained. Covariates were imputed using chained equations (5 imputations, 10 iterations), accounting for their level of measurement. Socio-demographic factors were entered into all the chained equations. Continuous covariates were entered as outcomes in a series of linear regression models, while binary and categorical variables were entered into a series of multinomial logit regression models.

LASSO is a covariate selection methodology that is superior to both generalized linear models without covariate selection as well as the usually applied stepwise or backward elimination process.(Zou, 2006) In fact, stepwise selection is often trapped into a local optimal solution rather than the global optimal solution and backward elimination can be time-consuming given the large number of variables in the full model.(Zou, 2006) These methods often ignore stochastic errors or uncertainty incurred during variable selection, with the LASSO estimate being defined as:

$$\beta(\text{lasso}) = \arg min_{\beta} \| y - \sum_{j=1}^{p} x_j \beta_j \|^2 + \lambda \sum_{j=1}^{p} |\beta_j|$$

with λ being a nonnegative regularization parameter.(Zou, 2006) The second term of the equation termed the "l1 penalty" is a key portion of this equation that ensures the success of the lasso method of covariate selection. This method was shown to discover the right sparse representation of the model, given certain conditions. Nevertheless, this method can produce biased estimates for larger coefficients. Thus, there a number of scenarios whereby the LASSO can yield inconsistent results. Recent methods have shown that an adaptive version of the LASSO gave more consistent findings, particularly when compared with the nonnegative garotte, another popular variable selection technique.

In our modeling approach, we used this convex optimization technique with l_1 constraint known as adaptive LASSO as one of three methods to select the final linear regression models. The model is trained on a random half sample of the total population (first imputation out of 5) and validated against the other half sample to check robustness of findings, by comparing R^2 between samples. One model was selected among the cvLASSO, adaptive LASSO or minBIC LASSO, depending on how close the R^2 are between half-samples. This parsimonious model selected for NfL exposures, Log_e transformed, (measured at v_1 and v_2) as 2 potential outcomes is then run on the entire population and a backward elimination process is carried out to keep only significant covariates at type I error

= 0.10. Thus, the selected model through LASSO was used as a starting point for further backward elimination. Backward elimination was conducted on the imputed data for the entire sample, rather than the half sample for the first imputation.

In our analysis, the following LASSO models were selected, and the final model included is shown also in this Table.

Table IV.1. Results of LASSO selection models and backward elimination

	Selected covariates[1]			
	cvLASSO	**Min BIC LASSO**	**Adaptive LASSO**	**Reduced model**
NfL (v1)	Age, Race, BMI, current drug use, insulin, phosphate, Chlorine, CO2, poverty status, urinary specific gravity, creatinine, sex, potassium, lipase, platelets, education, self-rated health, Chol:HDL ratio, TIBC	Age, Race, Poverty Status, Sex	**Age, Race, BMI, current drug use, phosphate, CO2, Poverty status, urinary specific gravity, creatinine, Sex, lipase, platelets, education, Chol:HDL ratio, TIBC, albumin, HbA1C, self-rated health, 25(OH)D, HDL-cholesterol, glucose, LDL-cholesterol, ALT, LDH, Basophils as % total WBC, Blood urea nitrogen, Diabetes, amylase, TSH, hypertension, albumin:globulin ratio, CES-D total score, neutrophils, MCV, microalbumin**	**Age, Race, BMI, current drugs, poverty status, urinary specific gravity, creatinine, sex, albumin, self-rated health, 25(OH)D**
NfL (v2)	Age, Race, GGT, BMI, Creatinine, Chlorine, insulin, lipase, amylase, HbA1C, Poverty status, sex, self-rated health, NSAIDs, ALP, WHR, WBC, Neutrophils % total WBC, Urinary specific gravity, blood urea nitrogen, smoking, B12, self-rated health, RPR, CRP, HIV, hypertension	Age, Race, Poverty Status, Sex	**Age, Race, GGT, BMI, Creatinine, Chlroine, insulin, lipase, amylase, HbA1C, poverty status, sex, WHR, neutrophils as % WBC, urinary specific gravity, self-rated health, serum glucose, uric acid, eosinophils as % WBC, HDL-cholesterol, Diabetes, current drug sue, CES-D total score, ESR, LDH**	**Age, sex, race, poverty status, BMI, Creatinine, ALP, Urinary specific gravity, blood urea nitrogen, serum glucose, uric acid, eosinophils as % WBC, Diabetes**

Abbreviations: BIC=Bayesian information criterion; BMI=Body Mass Index; cv=cross-validation; CVD=Self-reported cardiovascular disease; LASSO= Least absolute shrinkage and selection operator; A full row of bolded sets of covariates indicates that the selection process is equivalent, and that backward elimination did not reduce the model further.

The final common set of covariates that were chosen using the reduced model for each exposure was:

NfL at v_1: Age, Race, BMI, current drugs, poverty status, urinary specific gravity, creatinine, sex, albumin, self-rated health, 25(OH)D

NfL at v_2: Age, sex, race, poverty status, BMI, Creatinine, ALP, Urinary specific gravity, blood urea nitrogen, serum glucose, uric acid, eosinophils as % WBC, Diabetes

From these, six models were constructed:

Model 1: Only socio-demographic

Model 2: Socio-demographic + BMI

Model 3: Socio-demographic +BMI + serum glucose+diabetes.

Model 4: Socio-demographic +BMI +kidney/liver disease markers (Creatinine, ALP, Urinary specific gravity, blood urea nitrogen, uric acid).

Model 5:Socio-demographic+BMI+inflammatory markers (25(OH)D, eosinophils as % WBC, albumin)

Model 6: Socio-demographic +BMI+lifestyle/health related factors (current drug use, self-rated health).

C. Full description of the modeling approach:

Using multiple imputed data (k=5 imputations), a sensitivity analysis (SA) adjusted for additional covariates, selected with a multi-step process detailed in **supplemental method 4**, that included machine learning, followed by backward elimination and finally selection of a common pool of covariates that were independent predictors of one of two exposures. The pool of covariates initially selected had exhibited associations with either NfL measures and/or cognitive outcomes in previous studies. Thus, the final modeling approach consisted of a minimally adjusted basic model i.e., **Model 1** conducted on the unimputed data. Subsequently, the SA was carried out on multiple imputed data, with the following modeling approach, running in a serial manner Models 2 through 6 described in **B**.

Supplemental References:

Beydoun, M.A., Beydoun, H.A., Mode, N., Dore, G.A., Canas, J.A., Eid, S.M., Zonderman, A.B., 2016a. Racial disparities in adult all-cause and cause-specific mortality among us adults: mediating and moderating factors. BMC Public Health 16(1), 1113.

Beydoun, M.A., Canas, J.A., Dore, G.A., Beydoun, H.A., Rostant, O.S., Fanelli-Kuczmarski, M.T., Evans, M.K., Zonderman, A.B., 2016b. Serum Uric Acid and Its Association with Longitudinal Cognitive Change Among Urban Adults. J Alzheimers Dis 52(4), 1415-1430.

Beydoun, M.A., Fanelli Kuczmarski, M.T., Beydoun, H.A., Shroff, M.R., Mason, M.A., Evans, M.K., Zonderman, A.B., 2010a. The sex-specific role of plasma folate in mediating the association of dietary quality with depressive symptoms. J Nutr 140(2), 338-347.
Beydoun, M.A., Hossain, S., Chitrala, K.N., Tajuddin, S.M., Beydoun, H.A., Evans, M.K., Zonderman, A.B., 2019a. Association between epigenetic age acceleration and depressive symptoms in a prospective cohort study of urban-dwelling adults. J Affect Disord 257, 64-73.
Beydoun, M.A., Hossain, S., Fanelli-Kuczmarski, M.T., Beydoun, H.A., Canas, J.A., Evans, M.K., Zonderman, A.B., 2018. Vitamin D Status and Intakes and Their Association With Cognitive Trajectory in a Longitudinal Study of Urban Adults. J Clin Endocrinol Metab 103(4), 1654-1668.
Beydoun, M.A., Obhi, H.K., Weiss, J., Canas, J.A., Beydoun, H.A., Evans, M.K., Zonderman, A.B., 2019b. Systemic inflammation is associated with depressive symptoms differentially by sex and race: a longitudinal study of urban adults. Mol Psychiatry.
Beydoun, M.A., Shaked, D., Tajuddin, S.M., Weiss, J., Evans, M.K., Zonderman, A.B., 2020. Accelerated epigenetic age and cognitive decline among urban-dwelling adults. Neurology 94(6), e613-e625.
Beydoun, M.A., Shroff, M.R., Beydoun, H.A., Zonderman, A.B., 2010b. Serum folate, vitamin B-12, and homocysteine and their association with depressive symptoms among U.S. adults. Psychosom Med 72(9), 862-873.
Blackwell, E., de Leon, C.F., Miller, G.E., 2006. Applying mixed regression models to the analysis of repeated-measures data in psychosomatic medicine. Psychosom Med 68(6), 870-878.
Diagnostics, Q., Ferritin. https://www.questdiagnostics.com/testcenter/TestDetail.action?ntc=457&searchString=8272. (Accessed May 13sth 2019).
Diagnostics, Q., Hemogram. https://www.questdiagnostics.com/testcenter/BUOrderInfo.action?tc=7008&labCode=DAL. (Accessed May 13sth 2019).
Diagnostics, Q., Iron, Total and Total Iron Binding Capacity. https://www.questdiagnostics.com/testcenter/BUOrderInfo.action?tc=7573&labCode=SEA. (Accessed May 13sth 2019).
Diagnostics, Q., Vitamin B-12 (cobalamin) and folate panel. https://testdirectory.questdiagnostics.com/test/test-detail/7065/vitamin-b12-cobalamin-and-folate-panel-serum?cc=MASTER. (Accessed October 21st 2019).
Doshi, J., Erus, G., Ou, Y., Gaonkar, B., Davatzikos, C., 2013. Multi-atlas skull-stripping. Acad Radiol 20(12), 1566-1576.
Doshi, J., Erus, G., Ou, Y., Resnick, S.M., Gur, R.C., Gur, R.E., Satterthwaite, T.D., Furth, S., Davatzikos, C., Alzheimer's Neuroimaging, I., 2016. MUSE: MUlti-atlas region Segmentation utilizing Ensembles of registration algorithms and parameters, and locally optimal atlas selection. Neuroimage 127, 186-195.
Fanelli Kuczmarski, M., Bodt, B.A., Stave Shupe, E., Zonderman, A.B., Evans, M.K., 2018. Dietary Patterns Associated with Lower 10-Year Atherosclerotic Cardiovascular Disease Risk among Urban African-American and White Adults Consuming Western Diets. Nutrients 10(2).
Fanelli Kuczmarski, M., Mason, M.A., Beydoun, M.A., Allegro, D., Zonderman, A.B., Evans, M.K., 2013. Dietary patterns and sarcopenia in an urban African American and White population in the United States. J Nutr Gerontol Geriatr 32(4), 291-316.

Gunter, J.L., Bernstein, M.A., Borowski, B.J., Ward, C.P., Britson, P.J., Felmlee, J.P., Schuff, N., Weiner, M., Jack, C.R., 2009. Measurement of MRI scanner performance with the ADNI phantom. Med Phys 36(6), 2193-2205.
Hisamatsu, T., Fujiyoshi, A., Miura, K., Ohkubo, T., Kadota, A., Kadowaki, S., Kadowaki, T., Yamamoto, T., Miyagawa, N., Zaid, M., Torii, S., Takashima, N., Murakami, Y., Okamura, T., Horie, M., Ueshima, H., Group, S.R., 2014. Lipoprotein particle profiles compared with standard lipids in association with coronary artery calcification in the general Japanese population. Atherosclerosis 236(2), 237-243.
Ispir, E., Serdar, M.A., Ozgurtas, T., Gulbahar, O., Akin, K.O., Yesildal, F., Kurt, I., 2015. Comparison of four automated serum vitamin B12 assays. Clin Chem Lab Med 53(8), 1205-1213.
Larsson, A., Hansson, L.O., 2004. Analysis of inflammatory response in human plasma samples by an automated multicapillary electrophoresis system. Clin Chem Lab Med 42(12), 1396-1400.
Li, C., Gore, J.C., Davatzikos, C., 2014. Multiplicative intrinsic component optimization (MICO) for MRI bias field estimation and tissue segmentation. Magn. Reson. Imaging 32(7), 913-923.
Manickam, P., Rathod, A., Panaich, S., Hari, P., Veeranna, V., Badheka, A., Jacob, S., Afonso, L., 2011. Comparative prognostic utility of conventional and novel lipid parameters for cardiovascular disease risk prediction: do novel lipid parameters offer an advantage? Journal of clinical lipidology 5(2), 82-90.
Mayo Clinic, 2017. Sed rate (erythrocyte sedimentation rate). https://www.mayoclinic.org/tests-procedures/sed-rate/about/pac-20384797. (Accessed May 10th 2019).
Mellen, P.B., Gao Sk Fau - Vitolins, M.Z., Vitolins Mz Fau - Goff, D.C., Jr., Goff, D.C., Jr., Deteriorating dietary habits among adults with hypertension: DASH dietary accordance, NHANES 1988-1994 and 1999-2004. (0003-9926 (Print)).
Mulkern, R.V., Forbes, P., Dewey, K., Osganian, S., Clark, M., Wong, S., Ramamurthy, U., Kun, L., Poussaint, T.Y., 2008. Establishment and results of a magnetic resonance quality assurance program for the pediatric brain tumor consortium. Acad Radiol 15(9), 1099-1110.
Murakami, K., Livingstone, M.B.E., Sasaki, S., 2019. Diet quality scores in relation to metabolic risk factors in Japanese adults: a cross-sectional analysis from the 2012 National Health and Nutrition Survey, Japan. Eur J Nutr 58(5), 2037-2050.
Murphy, S.P., Foote, J.A., Wilkens, L.R., Basiotis, P.P., Carlson, A., White, K.K., Yonemori, K.M., 2006. Simple measures of dietary variety are associated with improved dietary quality. Journal of the American Dietetic Association 106(3), 425-429.
Myers, J.K., Weissman, M.M., 1980. Use of a self-report symptom scale to detect depression in a community sample. Am J Psychiatry 137(9), 1081-1084.
Nair, D., Carrigan, T.P., Curtin, R.J., Popovic, Z.B., Kuzmiak, S., Schoenhagen, P., Flamm, S.D., Desai, M.Y., 2009. Association of total cholesterol/ high-density lipoprotein cholesterol ratio with proximal coronary atherosclerosis detected by multislice computed tomography. Preventive cardiology 12(1), 19-26.
Nguyen, H.T., Kitner-Triolo, M., Evans, M.K., Zonderman, A.B., 2004. Factorial invariance of the CES-D in low socioeconomic status African Americans compared with a nationally representative sample. Psychiatry Res 126(2), 177-187.
Owen, W.E., Roberts, W.L., 2003. Comparison of five automated serum and whole blood folate assays. Am J Clin Pathol 120(1), 121-126.
phantom, N.d.

Powe, C.E., Evans, M.K., Wenger, J., Zonderman, A.B., Berg, A.H., Nalls, M., Tamez, H., Zhang, D., Bhan, I., Karumanchi, S.A., Powe, N.R., Thadhani, R., 2013. Vitamin D-binding protein and vitamin D status of black Americans and white Americans. N Engl J Med 369(21), 1991-2000.
Radloff, L., 1977. The CES-D scale: a self-report depression scale for research in the general population. Applied Psychological Measurement 1(385-401).
Ramos, M.I., Allen, L.H., Haan, M.N., Green, R., Miller, J.W., 2004. Plasma folate concentrations are associated with depressive symptoms in elderly Latina women despite folic acid fortification. Am J Clin Nutr 80(4), 1024-1028.
Samarina, T., Proskurnin, M., 2015. Rapid assessment of iron in blood plasma and serum by spectrophotometry with cloud-point extraction. F1000Res 4, 623.
Tajuddin, S.M., Hernandez, D.G., Chen, B.H., Noren Hooten, N., Mode, N.A., Nalls, M.A., Singleton, A.B., Ejiogu, N., Chitrala, K.N., Zonderman, A.B., Evans, M.K., 2019. Novel age-associated DNA methylation changes and epigenetic age acceleration in middle-aged African Americans and whites. Clin Epigenetics 11(1), 119.
techs, O.l.c.e.f.c.l.a.m., 2019. Red Blood Cell Distribution Width (RDW): Definition and Calculation.
Waldstein, S.R., Dore, G.A., Davatzikos, C., Katzel, L.I., Gullapalli, R., Seliger, S.L., Kouo, T., Rosenberger, W.F., Erus, G., Evans, M.K., Zonderman, A.B., 2017. Differential Associations of Socioeconomic Status With Global Brain Volumes and White Matter Lesions in African American and White Adults: the HANDLS SCAN Study. Psychosom Med 79(3), 327-335.
Wolters, M., Hickstein, M., Flintermann, A., Tewes, U., Hahn, A., 2005. Cognitive performance in relation to vitamin status in healthy elderly German women-the effect of 6-month multivitamin supplementation. Prev Med 41(1), 253-259.
Yin, W., Xu, Z., Sheng, J., Xie, X., Zhang, C., 2017. Erythrocyte sedimentation rate and fibrinogen concentration of whole blood influences the cellular composition of platelet-rich plasma obtained from centrifugation methods. Exp Ther Med 14(3), 1909-1918.
Zou, H., 2006. The adaptive Lasso and it oracle properties. Journal of the American Statistical Association 101(476), 1418-1428.

Online Supplementary Results 1

Similarly, **Table S2** explores those same study characteristics distributions in the total population, across NfL exposure tertiles (i.e. Log_e transformed plasma NfL, at v_1 and v_2). Generally, baseline age was directly related to NfL tertiles, with a 11-12y difference in mean age between the lowest and uppermost tertile. Percent above poverty was more elevated in the uppermost tertile of NfL at v_1 vs. lowest tertile (83.1% vs. 56.7%), but not at v_2. In contrast, mean BMI was lower in the uppermost tertile of NfL at v_1 vs. the lowest tertile (30.9 vs. 27.6, $P_{trend}<0.01$), a relationship that remained significant after further adjustment for age, sex, race and poverty status. While several lifestyle, health-related and laboratory indices were either directly or inversely related to NfL tertile, only a few remained significant correlates after adjustment for age, sex, race and poverty status. Specifically, alkaline phosphatase was directly related to NfL tertile at v_2 with a mean of 83.0 in the uppermost tertile vs. 69.3 in the lowest ($P_{trend}<0.001$), while 25(OH)D was inversely related to NfL tertile at v_1, with a mean of 26.4 in the uppermost tertile vs. 18.5 in the lowest ($P_{trend}<0.001$). NfL tertile at v_1 was directly related to WMLV after adjustment for age, sex, race, poverty status and ICV ($P_{trend}<0.010$). All other bivariate associations between NfL tertiles and sMRI measures, including hippocampal volumes, were attenuated with addition of socio-demographic factors.

Table S1. ROIs included in the small ROI volumes analyses (Analysis A") and WMLV analysis C' : volcano plots and FSLEYES analyses[a]

SMALL ROI VOLUMES	SMALL ROI WMLV
3rd.Ventricle_volM2	**3rd.Ventricle_wmlM2**
4th.Ventricle_volM2	**4th.Ventricle_wmlM2**
Right.Accumbens.Area_volM2	**Right.Accumbens.Area_wmlM2**
Left.Accumbens.Area_volM2	**Left.Accumbens.Area_wmlM2**
Right.Amygdala_volM2	Right.Amygdala_wmlM2
Left.Amygdala_volM2	Left.Amygdala_wmlM2
Brain.Stem_volM2	**Brain.Stem_wmlM2**
Right.Caudate_volM2	**Right.Caudate_wmlM2**
Left.Caudate_volM2	**Left.Caudate_wmlM2**
Right.Cerebellum.Exterior_volM2	**Right.Cerebellum.Exterior_wmlM2**
Left.Cerebellum.Exterior_volM2	Left.Cerebellum.Exterior_wmlM2
Right.Cerebellum.White.Matter_volM2	Right.Cerebellum.White.Matter_wmlM2
Left.Cerebellum.White.Matter_volM2	Left.Cerebellum.White.Matter_wmlM2
Right.Hippocampus_volM2	**Right.Hippocampus_wmlM2**
Left.Hippocampus_volM2	**Left.Hippocampus_wmlM2**
Right.Inf.Lat.Vent_volM2	**Right.Inf.Lat.Vent_wmlM2**
Left.Inf.Lat.Vent_volM2	**Left.Inf.Lat.Vent_wmlM2**
Right.Lateral.Ventricle_volM2	**Right.Lateral.Ventricle_wmlM2**
Left.Lateral.Ventricle_volM2	**Left.Lateral.Ventricle_wmlM2**
Right.Pallidum_volM2	Right.Pallidum_wmlM2
Left.Pallidum_volM2	Left.Pallidum_wmlM2
Right.Putamen_volM2	**Right.Putamen_wmlM2**
Left.Putamen_volM2	**Left.Putamen_wmlM2**
Right.Thalamus.Proper_volM2	**Right.Thalamus.Proper_wmlM2**
Left.Thalamus.Proper_volM2	**Left.Thalamus.Proper_wmlM2**
Right.Ventral.DC_volM2	**Right.Ventral.DC_wmlM2**
Left.Ventral.DC_volM2	**Left.Ventral.DC_wmlM2**
Cerebellar.Vermal.Lobules.I-V_volM2	Cerebellar.Vermal.Lobules.I-V_wmlM2
Cerebellar.Vermal.Lobules.VI-VII_volM2	Cerebellar.Vermal.Lobules.VI-VII_wmlM2
Cerebellar.Vermal.Lobules.VIII-X_volM2	Cerebellar.Vermal.Lobules.VIII-X_wmlM2
Left.Basal.Forebrain_volM2	**Left.Basal.Forebrain_wmlM2**
Right.Basal.Forebrain_volM2	Right.Basal.Forebrain_wmlM2
frontal.lobe.WM.right_volM2	**frontal.lobe.WM.right_wmlM2**
frontal.lobe.WM.left_volM2	**frontal.lobe.WM.left_wmlM2**
occipital.lobe.WM.right_volM2	**occipital.lobe.WM.right_wmlM2**
occipital.lobe.WM.left_volM2	**occipital.lobe.WM.left_wmlM2**
parietal.lobe.WM.right_volM2	**parietal.lobe.WM.right_wmlM2**

parietal.lobe.WM.left_volM2	**parietal.lobe.WM.left_wmlM2**
temporal.lobe.WM.right_volM2	**temporal.lobe.WM.right_wmlM2**
temporal.lobe.WM.left_volM2	**temporal.lobe.WM.left_wmlM2**
fornix.right_volM2	**fornix.right_wmlM2**
fornix.left_volM2	**fornix.left_wmlM2**
anterior.limb.of.internal.capsule.right_volM2	**anterior.limb.of.internal.capsule.right_wmlM2**
anterior.limb.of.internal.capsule.left_volM2	**anterior.limb.of.internal.capsule.left_wmlM2**
posterior.limb.of.internal.capsule.inc..cerebral.peduncle.right_volM2	**posterior.limb.of.internal.capsule.inc..cerebral.pedunc**
posterior.limb.of.internal.capsule.inc..cerebral.peduncle.left_volM2	**posterior.limb.of.internal.capsule.inc..cerebral.pedunc**
corpus.callosum_volM2	**corpus.callosum_wmlM2**
Right.ACgG.anterior.cingulate.gyrus_volM2	**Right.ACgG.anterior.cingulate.gyrus_wmlM2**
Left.ACgG.anterior.cingulate.gyrus_volM2	Left.ACgG.anterior.cingulate.gyrus_wmlM2
Right.AIns.anterior.insula_volM2	**Right.AIns.anterior.insula_wmlM2**
Left.AIns.anterior.insula_volM2	Left.AIns.anterior.insula_wmlM2
Right.AOrG.anterior.orbital.gyrus_volM2	**Right.AOrG.anterior.orbital.gyrus_wmlM2**
Left.AOrG.anterior.orbital.gyrus_volM2	Left.AOrG.anterior.orbital.gyrus_wmlM2
Right.AnG.angular.gyrus_volM2	**Right.AnG.angular.gyrus_wmlM2**
Left.AnG.angular.gyrus_volM2	Left.AnG.angular.gyrus_wmlM2
Right.Calc.calcarine.cortex_volM2	**Right.Calc.calcarine.cortex_wmlM2**
Left.Calc.calcarine.cortex_volM2	**Left.Calc.calcarine.cortex_wmlM2**
Right.CO.central.operculum_volM2	Right.CO.central.operculum_wmlM2
Left.CO.central.operculum_volM2	Left.CO.central.operculum_wmlM2
Right.Cun.cuneus_volM2	**Right.Cun.cuneus_wmlM2**
Left.Cun.cuneus_volM2	Left.Cun.cuneus_wmlM2
Right.Ent.entorhinal.area_volM2	Right.Ent.entorhinal.area_wmlM2
Left.Ent.entorhinal.area_volM2	Left.Ent.entorhinal.area_wmlM2
Right.FO.frontal.operculum_volM2	Right.FO.frontal.operculum_wmlM2
Left.FO.frontal.operculum_volM2	Left.FO.frontal.operculum_wmlM2
Right.FRP.frontal.pole_volM2	Right.FRP.frontal.pole_wmlM2
Left.FRP.frontal.pole_volM2	Left.FRP.frontal.pole_wmlM2
Right.FuG.fusiform.gyrus_volM2	Right.FuG.fusiform.gyrus_wmlM2
Left.FuG.fusiform.gyrus_volM2	Left.FuG.fusiform.gyrus_wmlM2
Right.GRe.gyrus.rectus_volM2	Right.GRe.gyrus.rectus_wmlM2
Left.GRe.gyrus.rectus_volM2	Left.GRe.gyrus.rectus_wmlM2
Right.IOG.inferior.occipital.gyrus_volM2	Right.IOG.inferior.occipital.gyrus_wmlM2
Left.IOG.inferior.occipital.gyrus_volM2	Left.IOG.inferior.occipital.gyrus_wmlM2
Right.ITG.inferior.temporal.gyrus_volM2	Right.ITG.inferior.temporal.gyrus_wmlM2
Left.ITG.inferior.temporal.gyrus_volM2	Left.ITG.inferior.temporal.gyrus_wmlM2
Right.LiG.lingual.gyrus_volM2	**Right.LiG.lingual.gyrus_wmlM2**
Left.LiG.lingual.gyrus_volM2	**Left.LiG.lingual.gyrus_wmlM2**
Right.LOrG.lateral.orbital.gyrus_volM2	Right.LOrG.lateral.orbital.gyrus_wmlM2

Left.LOrG.lateral.orbital.gyrus_volM2	Left.LOrG.lateral.orbital.gyrus_wmlM2
Right.MCgG.middle.cingulate.gyrus_volM2	Right.MCgG.middle.cingulate.gyrus_wmlM2
Left.MCgG.middle.cingulate.gyrus_volM2	Left.MCgG.middle.cingulate.gyrus_wmlM2
Right.MFC.medial.frontal.cortex_volM2	**Right.MFC.medial.frontal.cortex_wmlM2**
Left.MFC.medial.frontal.cortex_volM2	Left.MFC.medial.frontal.cortex_wmlM2
Right.MFG.middle.frontal.gyrus_volM2	Right.MFG.middle.frontal.gyrus_wmlM2
Left.MFG.middle.frontal.gyrus_volM2	Left.MFG.middle.frontal.gyrus_wmlM2
Right.MOG.middle.occipital.gyrus_volM2	**Right.MOG.middle.occipital.gyrus_wmlM2**
Left.MOG.middle.occipital.gyrus_volM2	Left.MOG.middle.occipital.gyrus_wmlM2
Right.MOrG.medial.orbital.gyrus_volM2	**Right.MOrG.medial.orbital.gyrus_wmlM2**
Left.MOrG.medial.orbital.gyrus_volM2	Left.MOrG.medial.orbital.gyrus_wmlM2
Right.MPoG.postcentral.gyrus.medial.segment_volM2	Right.MPoG.postcentral.gyrus.medial.segment_wmlM2
Left.MPoG.postcentral.gyrus.medial.segment_volM2	Left.MPoG.postcentral.gyrus.medial.segment_wmlM2
Right.MPrG.precentral.gyrus.medial.segment_volM2	Right.MPrG.precentral.gyrus.medial.segment_wmlM2
Left.MPrG.precentral.gyrus.medial.segment_volM2	Left.MPrG.precentral.gyrus.medial.segment_wmlM2
Right.MSFG.superior.frontal.gyrus.medial.segment_volM2	Right.MSFG.superior.frontal.gyrus.medial.segment_wml
Left.MSFG.superior.frontal.gyrus.medial.segment_volM2	Left.MSFG.superior.frontal.gyrus.medial.segment_wmlM
Right.MTG.middle.temporal.gyrus_volM2	Right.MTG.middle.temporal.gyrus_wmlM2
Left.MTG.middle.temporal.gyrus_volM2	Left.MTG.middle.temporal.gyrus_wmlM2
Right.OCP.occipital.pole_volM2	Right.OCP.occipital.pole_wmlM2
Left.OCP.occipital.pole_volM2	Left.OCP.occipital.pole_wmlM2
Right.OFuG.occipital.fusiform.gyrus_volM2	Right.OFuG.occipital.fusiform.gyrus_wmlM2
Left.OFuG.occipital.fusiform.gyrus_volM2	Left.OFuG.occipital.fusiform.gyrus_wmlM2
Right.OpIFG.opercular.part.of.the.inferior.frontal.gyrus_volM2	Right.OpIFG.opercular.part.of.the.inferior.frontal.gyrus_
Left.OpIFG.opercular.part.of.the.inferior.frontal.gyrus_volM2	Left.OpIFG.opercular.part.of.the.inferior.frontal.gyrus_w
Right.OrIFG.orbital.part.of.the.inferior.frontal.gyrus_volM2	Right.OrIFG.orbital.part.of.the.inferior.frontal.gyrus_wm
Left.OrIFG.orbital.part.of.the.inferior.frontal.gyrus_volM2	Left.OrIFG.orbital.part.of.the.inferior.frontal.gyrus_wml
Right.PCgG.posterior.cingulate.gyrus_volM2	Right.PCgG.posterior.cingulate.gyrus_wmlM2
Left.PCgG.posterior.cingulate.gyrus_volM2	Left.PCgG.posterior.cingulate.gyrus_wmlM2
Right.PCu.precuneus_volM2	**Right.PCu.precuneus_wmlM2**
Left.PCu.precuneus_volM2	Left.PCu.precuneus_wmlM2
Right.PHG.parahippocampal.gyrus_volM2	Right.PHG.parahippocampal.gyrus_wmlM2
Left.PHG.parahippocampal.gyrus_volM2	Left.PHG.parahippocampal.gyrus_wmlM2
Right.PIns.posterior.insula_volM2	Right.PIns.posterior.insula_wmlM2
Left.PIns.posterior.insula_volM2	**Left.PIns.posterior.insula_wmlM2**
Right.PO.parietal.operculum_volM2	**Right.PO.parietal.operculum_wmlM2**
Left.PO.parietal.operculum_volM2	Left.PO.parietal.operculum_wmlM2
Right.PoG.postcentral.gyrus_volM2	**Right.PoG.postcentral.gyrus_wmlM2**
Left.PoG.postcentral.gyrus_volM2	Left.PoG.postcentral.gyrus_wmlM2
Right.POrG.posterior.orbital.gyrus_volM2	Right.POrG.posterior.orbital.gyrus_wmlM2
Left.POrG.posterior.orbital.gyrus_volM2	Left.POrG.posterior.orbital.gyrus_wmlM2

Right.PP.planum.polare_volM2	Right.PP.planum.polare_wmlM2
Left.PP.planum.polare_volM2	Left.PP.planum.polare_wmlM2
Right.PrG.precentral.gyrus_volM2	**Right.PrG.precentral.gyrus_wmlM2**
Left.PrG.precentral.gyrus_volM2	Left.PrG.precentral.gyrus_wmlM2
Right.PT.planum.temporale_volM2	Right.PT.planum.temporale_wmlM2
Left.PT.planum.temporale_volM2	Left.PT.planum.temporale_wmlM2
Right.SCA.subcallosal.area_volM2	Right.SCA.subcallosal.area_wmlM2
Left.SCA.subcallosal.area_volM2	Left.SCA.subcallosal.area_wmlM2
Right.SFG.superior.frontal.gyrus_volM2	Right.SFG.superior.frontal.gyrus_wmlM2
Left.SFG.superior.frontal.gyrus_volM2	**Left.SFG.superior.frontal.gyrus_wmlM2**
Right.SMC.supplementary.motor.cortex_volM2	Right.SMC.supplementary.motor.cortex_wmlM2
Left.SMC.supplementary.motor.cortex_volM2	**Left.SMC.supplementary.motor.cortex_wmlM2**
Right.SMG.supramarginal.gyrus_volM2	**Right.SMG.supramarginal.gyrus_wmlM2**
Left.SMG.supramarginal.gyrus_volM2	Left.SMG.supramarginal.gyrus_wmlM2
Right.SOG.superior.occipital.gyrus_volM2	**Right.SOG.superior.occipital.gyrus_wmlM2**
Left.SOG.superior.occipital.gyrus_volM2	Left.SOG.superior.occipital.gyrus_wmlM2
Right.SPL.superior.parietal.lobule_volM2	Right.SPL.superior.parietal.lobule_wmlM2
Left.SPL.superior.parietal.lobule_volM2	Left.SPL.superior.parietal.lobule_wmlM2
Right.STG.superior.temporal.gyrus_volM2	Right.STG.superior.temporal.gyrus_wmlM2
Left.STG.superior.temporal.gyrus_volM2	Left.STG.superior.temporal.gyrus_wmlM2
Right.TMP.temporal.pole_volM2	Right.TMP.temporal.pole_wmlM2
Left.TMP.temporal.pole_volM2	Left.TMP.temporal.pole_wmlM2
Right.TrIFG.triangular.part.of.the.inferior.frontal.gyrus_volM2	Right.TrIFG.triangular.part.of.the.inferior.frontal.gyrus_v
Left.TrIFG.triangular.part.of.the.inferior.frontal.gyrus_volM2	Left.TrIFG.triangular.part.of.the.inferior.frontal.gyrus_wr
Right.TTG.transverse.temporal.gyrus_volM2	Right.TTG.transverse.temporal.gyrus_wmlM2
Left.TTG.transverse.temporal.gyrus_volM2	Left.TTG.transverse.temporal.gyrus_wmlM2

[a] Note than only 61 ROIs were included in analysis C', given that all others were null for all participants. Those are the bolded and red ROIs for WMLV. Further filtering was made at a level of 5% non-zero or more (n=24). Since all ROIs were included for volumetric ROI-specific analysis (Analysis A"), those are all bolded.

Table S2. Study sample characteristics of eligible study sample by NfL(v1) and NfL(v2) tertiles, overall; HANDLS 2004-2009/2009-2013 (NfL at v_1 and v_2) and HANDLS-SCAN 2011-2015[a]

	NfL at v1			*Nfl at v2*		
	T1	*T2*	*T3*	*T1*	*T2*	*T3*
	(N=60)	*(N=60)*	*(N=59)*	*(N=60)*	*(N=60)*	*(N=59)*
Plasma NfL						
NfL at v_1, Log_e transformed						
Mean±SD	1.49±0.28	1.99±0.11	2.57±0.41***	1.57±0.36	2.087±0.408	2.386±0.450***
IQR	1.37-1.67	1.92-2.09	2.26-2.68	1.37-1.84	1.85-2.24	2.11-2.64
NfL at v_2, Log_e transformed						
Mean±SD	1.81±0.43	2.25±0.54	2.60±0.47***	1.662±0.247	2.168±0.102	2.831±0.498***
IQR	1.57-2.02	1.79-2.37	2.23-2.83	1.47-1.85	2.08-2.25	2.56-2.99
"Tracking high" v_1 through v_2: NfL>8 pg/mL	0.0	18.0	91.0***	0.0	32.0	78.0***
"Tracking low", v_1 through v_2: NfL≤8 pg/mL	80.0	28.0	0.0***	93.0	15.0	0.0***
Socio-demographic factors						
Sex, % males	40.0	48.3	45.8	43.3	41.7	49.2
Age_{v1}	41.9±7.9	47.6±8.4	53.9±6.7***	41.8±7.5	47.6±8.0	54.0±7.4***
Race, % AA	50.0	40.0	33.9	55.0	36.7	32.2*
% above poverty	56.7	66.7	83.1**	60.0	73.3	72.9
Time between v_1 and v_{scan} (days)	2,103±618	1858± 658	1973± 609	1,992±666	1,860±621	2,083± 602
Time between v_2 and v_{scan}(days)	487±471	333±392	413±455	447± 479	334±374	453±465
Imputed covariates, % or Mean±SE						
Body mass index, $kg.m^{-2}$	30.9±0.9	29.4±0.8	27.6±0.7**, b	30.0±0.9	29.4±0.8	28.6±0.8
Diabetes						
No	74.7	69.0	72.2	74.0	71.3	69.5
Pre-diabetes	17.0	20.3	15.6	17.3	17.0	18.6
Diabetes	8.3	11.7	12.2	8.7	11.7	11.9
Plasma glucose, mg/dL	97.5± 3.1	99.6±2.6	102.7±4.9	97.1±3.0	97.5± 2.4	105.2±4.9
Creatinine, mg/dL	0.87±0.04	0.89±0.04	0.92±0.04	0.88±0.04	0.86±0.03	0.94±0.02
Urine Specific Gravity	1.019±0.0010	1.020±0.0007	1.018±0.0008	1.0197±0.0010	1.019 ±0.0006	1.019±0.0008
Blood urea nitrogen, mg/dL	12.7±0.5	14.03±0.517	14.56±0.56*	12.50±0.54	13.57±0.40	15.20±0.61***
Alkaline Phosphatase, U/L	70.9±2.4	74.6±3.1	80.2±2.4*	69.3±2.7	73.5±2.2	83.0 ±2.9***,b

Uric acid, mg/dL	5.36±0.17	5.79±0.24	5.33 ±0.15 [b]	5.40±0.17	5.44±0.21	5.64±0.18
Albumin, g/dL	4.35±0.04	4.38±0.03	4.30±0.03	4.34±0.04	4.36±0.04	4.32±0.03
Eosinophils, %	2.72±0.22	2.74±0.24	2.78±0.30	2.62±0.23	2.73±0.27	2.89±0.27
25-hydroxyvitamin D, ng/mL	18.5±1.2	22.2±1.5	26.4±1.6***, [b]	18.3±1.3	23.93±1.63	24.81±1.25**
Current drug use, % yes	17.3	17.0	26.1	19.0	23.3	18.0
Self-rated health, %						
Poor/fair	18.3	25.0	22.0	23.3	20.0	22.0
Good	38.3	31.7	40.7	36.7	40.0	33.9
Very good/Excellent	43.4	43.3	37.3	40.0	40.0	44.1
sMRI measures						
Intracranial volume, mm^3(mean±SD)	1,327,429±130,020	1,344,990±148,920	1,345,624±148,282	1,333,967±147,315	1,327,240 ±130,181	1,357,026±148,825
Global cortical brain volumes,* mm^3 *(mean±SD)						
Total brain volume	1,147,025±107,813	1,144,965±131,262	1,136,569±115,739	1,153,259±123,664	1,132,592± 108,305	1,142,813±122,879
Gray Matter	650,352±61,813	644,497±72,860	632,217±59,947	654,670±67,051	636,968± 62,593	635,484±65,285
White Matter	456,429±47,309	458,894±58,998	456,464±52,520	458805±56111	453,604± 47,453	459,429±55,368
***Regional cortical brain volumes,* mm^3 *(mean±SD*)**						
Left Brain						
Frontal GM	95,041±9,466	93,621±10,931	90,943± 9,581*	95,524±9,916	92,329± 10,088	91,765±10,067 *
Frontal WM	85,443±9,303	85,499±11,285	85,030±10,487	85,757±10,817	84,499± 9,541	85,728±10,724
Temporal GM	50,490±5,751	50,786±6,932	49,580±5,690	50,700±6,471	50,225± 5,847	49,936±6,166
Temporal WM	49,119±5,434	49,613±6,900	49,367± 6,015	49,375±6,731	48,983± 5,437	49,747±6,190
Parietal GM	46,756±5,186	46,169± 6,383	45,511± 5,404	47,239±5,675	45,918± 5,437	45,275±5,823
Parietal WM	43,539±4,818	44,201± 6,108	43,953±5,899	43,790±5,723	43,590± 4,932	44,318±6,184
Occipital GM	38,345±4,629	38,574±6,186	37,293±4,690	38,622±5,117	38,286± 5,049	37,304±5,490
Occipital WM	20,893±2,808	21,361±3,143	20,827±2,932	21,123±3,052	21,081± 2,652	20,878±3,190
Right Brain						
Frontal GM	95,162±9,996	93,666±11,204	91,033±9,397*	95,774±10,377	92,076± 10,122	92,029±10,165*
Frontal WM	87,669± 9,819	87,598±11,557	87,386±10,794	88,059±11,292	86,520±9,607	88,086±11,191

Temporal GM	51,615±5,867	51,881±6,486	50,149±5,577	51,823±6,186	51,021± 5,952	50,811±5,928
Temporal WM	49,825±5,473	50,195±6,841	49,716±5,855	50,123±6,468	49,504± 5,555	50,114± 6,187
Parietal GM	47,582±5,241	46,855±6,437	45,866±5,471	48,027±5,569	46,319± 5,383	45,958±6,164*
Parietal WM	41,351±4,709	41,924±5,982	41,779 ±5,665	41,620±5,545	41,468±4,900	41,968±5,949
Occipital GM	39038±4,898	39,733±6,087	39,233±5,215	39,541±5,470	39,529± 5,313	38,929±5,492
Occipital WM	20,441±2,768	21,016±3,042	20,993±2,990	20,692±3,029	20,762± 2,842	20996±2959
Hippocampal volume, mm^3						
Hippocampus, Left	3,559±391	3,553±400	3,499±368	3,543±416	3,603±345	3,464±386*
Hippocampus, Right	3,850±424	3,836±439	3,797±380	3,847±460	3,841±364	3,794±415
Hippocampus, Left, as % TBV	0.269±0.022	0.265±0.026	0.261±0.024	0.266±0.019	0.273±0.023	0.256±0.027
Hippocampus, Right, as % TBV	0.291±0.024	0.286±0.025	0.284±0.024	0.290±0.021	0.290± 0.026	0.281±0.026
White matter lesion volume, mm^3, Log$_e$ transformed	4.325±6.254	6.129±1.143	6.505±1.161**[,b]	4.689±5.451	6.249± 1.275	6.013±3.452
White matter lesion volume, mm^3, % TBV, Log$_e$ transformed	-5.164±6.243	-3.372±1.148	-2.996±1.152**[,b]	-4.804±5.433	-3.240± 1.254	-3.497±3.464

Abbreviations: Age$_{v1}$=age measured at HANDLS visit 1 (2004-2009); CV=Coefficient of Variation; IQR=Interquartile Range; GM=Gray Matter; HANDLS=Healthy Aging in Neighborhoods of Diversity Across the Life Span; HANDLS-SCAN=Brain magnetic resonance imaging scan ancillary study of HANDLS; IQR=Interquartile range (25th-75th percentile); NfL=Neurofilament Light; sMRI=Structural Magnetic Resonance Imaging; T1-T3=tertiles; v_1=visit 1 of HANDLS (2004-2009); v2=visit 2 of HANDLS (2009-2013); v_{scan}=HANDLS-SCAN visit (2011-2015); WM=White Matter.

[a] Values are Mean±SD (Mean±SE for imputed covariates), or %. Volumes are expressed in mm^3.

[b] P<0.05 after further adjustment for age, sex, race, poverty status for socio-demographic and sMRI measures.

*P<0.05 **P<0.010 ***P<0.001 for null hypothesis of no trend across tertiles of NfL, Log$_e$ transformed, tertiles.

Table S3. Selected covariate-adjusted associations from analyses A (global GM and WM volumes), A' (regional cortical GM/WM), B (hippocampal volume) and C (White matter lesion volume) vs. visit 1 NfL (overall and stratified by sex): ordinary least square analyses; HANDLS 2004-2009 and HANDLS-SCAN 2011-2015: Sensitivity analyses[a]

	Model 3		*Model 4*		*Model 5*		*Model 6*	
Total sample (N=179)	*β3*	*(SE3)*	*β4*	*(SE4)*	*β5*	*(SE5)*	*β6*	*(SE6)*
sMRI, Analysis A								
Total brain	+298	(17,228)	-4,752	(16,520)	-2,779	(17,177)	+8,533	(17,078)
GM	-5,805	(9,203)	-7,780	(8,952)	-4,429	(9,214)	+1,544	(9,106)
WM	+2,738	(8,400)	+561	(8,038)	+44	(8,336)	+3,722	(8,345)
sMRI, Analysis B								
Hippocampus, Left	-56.4	(56.3)	-46.1	(56.0)	-30.3	(56.3)	-46.8	(56.3)
Hippocampus, Right	-52.3	(57.8)	-47.1	(57.6)	-9.7	(58.1)	-36.3	(58.1)
Analysis C								
White matter lesion volume, Log_e transformed	**+2.508**	**(0.712)[e, f]**	**+2.347**	**(0.708)[e, f]**	**+2.56**	**(0.71)[e,f]**	**+2.300**	**(0.712)[e,f]**
Males (N=80)								
sMRI, Analysis A								
Total brain	-5,017	(26,145)	-20,634	(26,292)	-11,789	(26,211)	-6,189	(26,185)
GM	-10,677	(13,628)	-19,117	(13,669)	-10,592	(13,605)	-7,201	(13,546)
WM	-1,054	(12,708)	-5,860	(12,804)	-5,827	(12,745)	-4,182	(12,735)
sMRI, Analysis B								
Hippocampus, Left	-106.6	(80.7)	-86.6	(86.0)	-104.7	(81.6)	-30.5	(78.8)
Hippocampus, Right	-86.0	(81.1)	-93.5	(85.7)	-66.1	(83.3)	-2.5	(81.3)
Analysis C								
White matter lesion volume, Log_e transformed	**+1.58**	**(0.76)[d]**	**+1.94**	**(0.77)[d]**	+1.41	(0.76)[c]	+1.36	(0.76)[c]
Females (N=99)								
sMRI, Analysis A								

Total brain	12,621	(23,535)	+21,124	(21,927)	+17,345	(23,864)	+34,749	(22,913)
GM	4,233	(13,000)	+9,706	(12,492)	+8,932	(13,210)	+17,400	(12,794)
WM	11,325	(11,481)	+13,332	(10,532)	+11,997	(11,524)	+18,537	(11,155)
sMRI, Analysis B								
Hippocampus, Left	+56.1	(78.9)	+70.1	(78.3)	+110.7	(79.1)	+29.0	(79.1)
Hippocampus, Right	18.3	(86.1)	+25.4	(85.6)	+70.6	(85.4)	-25.2	(85.4)
Analysis C								
White matter lesion volume, Log_e transformed	**+4.33**	**(1.27)** [e]	**+3.96**	**(1.25)** [e]	**+4.47**	**(1.27)**[e]	**+3.76**	**(1.30)** [e]

Abbreviations: Age_{v1}=age measured at HANDLS visit 1 (2004-2009); GM=Gray Matter; HANDLS=Healthy Aging in Neighborhoods of Diversity Across the Life Span; HANDLS-SCAN=Brain magnetic resonance imaging scan ancillary study of HANDLS; NfL=Neurofilament Light Chain; SE=Standard Error; sMRI=Structural Magnetic Resonance Imaging; v_1=visit 1 of HANDLS (2004-2009); v2=visit 2 of HANDLS (2009-2013); v_{scan}=HANDLS-SCAN visit (2011-2015); WM=White Matter

[a] Values are adjusted linear regression coefficients β with associated SE. (N) is the sample size in each analysis. Model 2 in Table 2 was adjusted for Age_{v1}, sex, race, poverty status and time of follow-up between visit 1 and v_{scan} and BMI. Volumes are expressed in mm^3.

[b] Model 3 is a sensitivity analysis further adjusting Model 2 (Table 2) for Diabetes and serum glucose levels; Model 4 is a sensitivity analysis further adjusting Model 2 (Table 2) for selected markers of kidney and liver disease (creatinine, urinary specific gravity, blood urea nitrogen, alkaline phosphatase and uric acid); Model 5 is a sensitivity analysis further adjusting Model 2 (Table 2) for selected inflammatory factors (25-hydroxyvitamin D, serum albumin, eosinophils as % of total white blood cells); Model 6 is a sensitivity analysis further adjusting Model 2 (Table 2) for other lifestyle and health-related covariates (current drug use, self-rated health).

[c] $P<0.10$ [d] $P<0.05$ [e] $P<0.010$ for null hypothesis that exposure main effect is =0 in each model, stratified or unstratified.

[f] $P<0.10$ for null hypothesis that exposure×sex 2-way interaction term is =0 in the unstratified model with exposure and sex included as main effects.

Table S4. Selected covariate-adjusted associations from analyses A (global GM and WM volumes), A' (regional cortical GM/WM), B (hippocampal volume) and C (White matter lesion volume) vs. Visit 2 NfL (overall and stratified by sex): ordinary least square analyses; HANDLS 2009-2013 and HANDLS-SCAN 2011-2015: Sensitivity analyses[a]

	Model 3		*Model 4*		*Model 5*		*Model 6*	
Total sample (N=179)	*β3*	*(SE3)*	*β4*	*(SE4)*	*β5*	*(SE5)*	*β6*	*(SE6)*
sMRI, Analysis A								
Total brain	-4,558	(13,860)	-1,262	(13,622)	-3,969	(13,432)	-2,387	(13,314)
GM	-6,720	(7,397)	-6,186	(7,393)	-5,269	(7,208)	-4,339	(7,069)
WM	-1,416	(6.759)	+898	(6,637)	-1,682	(6,514)	-964	(6,505)
sMRI, Analysis B								
Hippocampus, Left	**-140.1**	**(44.1)[e]**	**-137.6**	**(45.3)[e]**	**-125.3**	**(42.9)[e]**	**-123.0**	**(42.9)[e]**
Hippocampus, Right	**-118.5**	**(45.7)[e]**	**-122.6**	**(46.8)[e]**	**-96.1**	**(44.9)[d]**	**-97.9**	**(44.7)[d]**
Analysis C								
White matter lesion volume, Log_e transformed	+0.48	(0.60)[f]	+0.38	(0.60)[f]	+0.47	(0.58)[f]	+0.471	(0.571)[f]
Males (N=80)								
sMRI, Analysis A								
Total brain	-15,062	(21,889)	-22,004	(21,340)	-17,661	(21,169)	-14,744	(21,431)
GM	-11,374	(11,421)	-15,548	(11,136)	-12,155	(11,005)	-9,783	(11,094)
WM	-7,185	(10,631)	-9,501	(10,398)	-8,266	(10,267)	-7,348	(10,396)
sMRI, Analysis B								
Hippocampus, Left	**-169.1**	**(65.6)[d]**	**-159.3**	**(68.1)[d]**	**-154.5**	**(64.4)[d]**	**-139.5**	**(62.1)[d]**
Hippocampus, Right	**-158.9**	**(66.0)[d]**	**-155.9**	**(68.1)[d]**	-123.4	(66.5)[c]	-127.6	(64.3)[c]
Analysis C								
White matter lesion volume, Log_e transformed	-0.274	(0.655)	-0.048	(0.660)	-0.270	(0.636)	-0.286	(0.637)
Females (N=99)								
sMRI, Analysis A								

Total brain	+7,701	(19,505)	+28,117	(19,772)	+11,430	(19,285)	14,539	(18,640)
GM	-2,561	(10,769)	+5,620	(11,313)	+888	(10,709)	2,346	(10,399)
WM	+8,453	(9,518)	+18,417	(9,472)[c]	+8,872	(9,319)	10,012	(9,076)
sMRI, Analysis B								
Hippocampus, Left	-40.9	(65.5)	-34.7	(71.9)	-17.9	(64.9)	-34.5	(63.2)
Hippocampus, Right	-29.6	(71.5)	-36.7	(78.3)	-11.1	(69.7)	-31.5	(68.3)
Analysis C								
White matter lesion volume, Log_e transformed	+1.68	(1.11)[f]	+1.39	(1.20)[f]	+1.63	(1.09)	+1.42	(1.08)

Abbreviations: Age_{v1}=age measured at HANDLS visit 1 (2004-2009); GM=Gray Matter; HANDLS=Healthy Aging in Neighborhoods of Diversity Across the Life Span; HANDLS-SCAN=Brain magnetic resonance imaging scan ancillary study of HANDLS; NfL=Neurofilament Light Chain; SE=Standard Error; sMRI=Structural Magnetic Resonance Imaging; v_1=visit 1 of HANDLS (2004-2009); v2=visit 2 of HANDLS (2009-2013); v_{scan}=HANDLS-SCAN visit (2011-2015); WM=White Matter.

[a] Values are adjusted linear regression coefficients β with associated SE. (N) is the sample size in each analysis. Model 2 in Table 3 was adjusted for Age_{v1}, sex, race, poverty status, intra-cranial volume for analyses B and C, and time of follow-up between visit 1 and v_{scan} and BMI. Volumes are expressed in mm^3.

[b] Model 3 is a sensitivity analysis further adjusting Model 2 (Table 3) for Diabetes and serum glucose levels; Model 4 is a sensitivity analysis further adjusting Model 2 (Table 3) for selected markers of kidney and liver disease (creatinine, urinary specific gravity, blood urea nitrogen, alkaline phosphatase and uric acid); Model 5 is a sensitivity analysis further adjusting Model 2 (Table 3) for selected inflammatory factors (25-hydroxyvitamin D, serum albumin, eosinophils as % of total white blood cells); Model 6 is a sensitivity analysis further adjusting Model 2 (Table 3) for other lifestyle and health-related covariates (current drug use, self-rated health).

[c] $P<0.10$ [d] $P<0.05$ [e] $P<0.010$ for null hypothesis that exposure main effect is =0 in each model, stratified or unstratified.

[f] $P<0.10$ for null hypothesis that exposure×sex 2-way interaction term is =0 in the unstratified model with exposure and sex included as main effects.

Table S5. Summary of findings from sensitivity analyses with NfL at v_1 and at v_2 (for hippocampal and lesion volume outcomes), adjusted for intracranial volume, by race HANDLS-SCAN 2011-2015

	NfL at v_1					
	Model 1	Model 2	Model 3	Model 4	Model 5	Model 6
	African Americans (n=74)					
Hippocampus, Left	-6.36±73.59 P=0.93	-38.00±85.82 P=0.66	-62.2±87.7 P=0.48	-32.4±94.7 P=0.73	-40.10±89.2 P=0.66	-15.31±87.36 P=0.86
Hippocampus, Right	+6.77±72.09 P=0.93	-40.77±83.6 P=0.63	-48.7±81.7 P=0.55	-45.4±90.8 P=0.62	-32.8±86.7 P=0.71	-13.25±85.48 P=0.88
Lesion volume, Log_e transformed	+1.61±0.84 P=0.061	**+2.36±0.97** **P=0.018**	**+2.37±1.04** **P=0.026**	**+2.28±1.03** **P=0.031**	**+2.37±1.02** **P=0.023**	+1.98±1.00 P=0.052
	Whites (n=105)					
Hippocampus, Left	-103.6±75.1 P=0.17	-94.0±74.7 P=0.21	-111.7±81.6 P=0.17	-106.0±78.0 P=0.18	-89.2±79.8 P=0.27	-107.0±78.2 P=0.18
Hippocampus, Right	-116.7±77.7 P=0.14	-103.5±76.6 P=0.18	-128.7±83.6 P=0.13	-127.3±80.0 P=0.12	-94.2±81.8 P=0.25	-124.3±80.0 P=0.12
Lesion volume, Log_e transformed	**+2.66±1.00** **P=0.009**	**+2.71±1.01** **P=0.008**	**+3.09±1.10** **P=0.006**	**+2.76±1.05** **P=0.010**	**+3.24±1.06** **P=0.003**	**+2.85±1.05** **P=0.008**
	NfL at v_2					
	Model 1	Model 2	Model 3	Model 4	Model 5	Model 6
	African Americans (n=74)					
Hippocampus, Left	-95.04±53.00 P=0.077	-103.2±53.8 P=0.060	**-136.6±54.3** **P=0.015**	-116.0±58.6 P=0.053	**-115.6±54.6** **P=0.038**	-104.3±52.8 P=0.053
Hippocampus, Right	-67.50±52.51	-78.7±53.0	**-107.2±50.6**	-99.3±57.2	-84.0±54.0	-78.5±52.3

	P=0.20	P=0.14	**P=0.038**	P=0.088	P=0.13	P=0.14
Lesion volume, Log_e transformed	+0.201±0.639 P=0.75	+0.241±0.652 P=0.71	+0.165±0.686 P=0.81	+0.259±0.702 P=0.71	+0.232±0.672 P=0.73	+0.174±0.641 P=0.79
	Whites (n=105)					
Hippocampus, Left	**-164.9±67.0** **P=0.016**	**-158.2±66.6** **P=0.020**	**-177.9±70.8** **P=0.014**	**-183.3±71.0** **P=0.011**	**-158.2±67.3** **P=0.021**	**-157.5±67.1** **P=0.021**
Hippocampus, Right	**-153.0±70.0** **P=0.031**	**-143.6±68.7** **P=0.039**	**-166.1±73.1** **P=0.025**	**-180.0±73.6** **P=0.017**	**-141.2±69.7** **P=0.046**	**-144.0±69.4** **P=0.041**
Lesion volume, Log_e transformed	+0.830±0.939 P=0.38	+0.853±0.945 P=0.37	+0.889±1.010 P=0.38	+0.622±1.011 P=0.54	+0.871±0.954 P=0.36	+0.838±0.951 P=0.38

Abbreviations: Age_{v1}=age measured at HANDLS visit 1 (2004-2009); HANDLS=Healthy Aging in Neighborhoods of Diversity Across the Life Span; HANDLS-SCAN=Brain magnetic resonance imaging scan ancillary study of HANDLS; NfL=Neurofilament Light; SE=Standard Error; v_1=visit 1 of HANDLS (2004-2009); v2=visit 2 of HANDLS (2009-2013); v_{scan}=HANDLS-SCAN visit (2011-2015).

[a] Values are adjusted linear regression coefficients β with associated SE. (N) is the sample size in each analysis. Volumes are expressed in mm^3.

[b] Model 1 adjusted for Age_{v1}, sex, poverty status, length of follow-up between v_1 and v_{scan} and intracranial volume (ICV). Model 2 is Model 1 further adjusted for BMI. Model 3 is a sensitivity analysis further adjusting Model 2 for Diabetes and serum glucose levels; Model 4 is a sensitivity analysis further adjusting Model 2 for selected markers of kidney and liver disease (creatinine, urinary specific gravity, blood urea nitrogen, alkaline phosphatase and uric acid); Model 5 is a sensitivity analysis further adjusting Model 2 for selected inflammatory factors (25-hydroxyvitamin D, serum albumin, eosinophils as % of total white blood cells); Model 6 is a sensitivity analysis further adjusting Model 2 for other lifestyle and health-related covariates (current drug use, self-rated health).

[c] P<0.10 for null hypothesis that exposure×race 2-way interaction term is =0 in the unstratified model with exposure and race included as main effects.

Table S6. Summary of findings from sensitivity analyses with NfL at v_1 and v_2 (for total brain, Gray Matter and White Matter volumes), by race HANDLS-SCAN 2011-2015

	NfL at v_1					
	Model 1	Model 2	Model 3	Model 4	Model 5	Model 6
	African Americans (n=74)					
Total brain	-42,535±23,258 [c] P=0.072	-47,311±27,615 [c] P=0.091	**-62,323±28,271** [c] **P=0.031**	-56,097±28,427 [c] P=0.053	-51,588±28,475 [c] P=0.075	-40,957±28,791 [c] P=0.16
Gray matter	-25,503±13,247 [c] P=0.058	-27,733±15,733 [c] P=0.083	**-38,762±15,912** [c] **P=0.018**	-32,888±16,461 [c] P=0.050	-28,055±16,300 [c] P=0.090	-20,177±16,183 [c] P=0.22
White matter	15,747±10,775 [c] P=0.15	-19,734±12,770 [c] P=0.13	-24,110±13,285 [c] P=0.074	-23,458±13,059 [c] P=0.078	-23,158±13,112 [c] P=0.082	-20,743±13,336 [c] P=0.13
	Whites (n=105)					
Total brain	+30,270±21,336 P=0.16	+31,171±21,488 P=0.15	+38,651±23,192 P=0.099	+21,520±21,772 P=0.33	+28,970±22,940 P=0.21	+36,303±22,273 P=0.11
Gray matter	+8,545±11,013 P=0.44	+9,370±11,060 P=0.40	+11,453±11,994 P=0.34	+4,643±11,362 P=0.68	+10,039±11,861 P=0.40	12,252±11,474 P=0.29
White matter	+16,599±10,783 P=0.13	16,860±10,869 P=0.12	+20,509±11,772 P=0.085	+12,833±11,032 P=0.25	+15,429±11,564 P=0.19	18,170±11,253 P=0.11
	NfL at v_2					
	Model 1	Model 2	Model 3	Model 4	Model 5	Model 6
	African Americans (n=74)					
Total brain	-18,548±17,918 P=0.30	-16,876±18,332 P=0.36	-26,585±18,846 P=0.16	-19,517±19,497 P=0.32	-20,992±18,608 P=0.26	-15,248±18,375 P=0.41

Gray matter	-10,746±10,229 P=0.30	-9,607±10,457 P=0.36	-16,393±10,558 P=0.13	+2,275±10,387 P=0.83	-11,545±10,665 P=0.28	-8,370±10,289 P=0.42
White matter	-8,375±8,232 P=0.31	-8,244±8,437 P=0.33	-11,337±8,815 P=0.20	+8,055±9,475 P=0.40	-10,227±8,529 P=0.24	-7,864±8,507 P=0.36
	Whites (n=105)					
Total brain	+11,911±19,691 P=0.55	+12,468±19,814 P=0.53	+15,833±20,980 P=0.45	+15,111±20,373 P=0.46	+11,458±20,030 P=0.57	+12,756±19,958 P=0.52
Gray matter	-383.7±10,112 P=0.97	+172±10,148 P=0.99	+667±10,780 P=0.95	-300±10,625 P=0.98	+27±10,325 P=1.00	+278±10,220 P=0.98
White matter	+7,226±9,961 P=0.47	+7,365±10,031 P=0.47	+8,928±10,657 P=0.40	+9,793±10,321 P=0.35	+6,683±10,101 P=0.51	+7,565±10,074 P=0.46

Abbreviations: Age_{v1}=age measured at HANDLS visit 1 (2004-2009); HANDLS=Healthy Aging in Neighborhoods of Diversity Across the Life Span; HANDLS-SCAN=Brain magnetic resonance imaging scan ancillary study of HANDLS; NfL=Neurofilament Light; SE=Standard Error; sMRI=Structural Magnetic Resonance Imaging; v_1=visit 1 of HANDLS (2004-2009); v2=visit 2 of HANDLS (2009-2013); v_{scan}=HANDLS-SCAN visit (2011-2015).

[a] Values are adjusted linear regression coefficients β with associated SE. (N) is the sample size in each analysis. Volumes are expressed in mm^3.

[b] Model 1 adjusted for Age_{v1}, sex, poverty status and length of follow-up between v_1 and v_{scan}. Model 2 is Model 1 further adjusted for BMI. Model 3 is a sensitivity analysis further adjusting Model 2 for Diabetes and serum glucose levels; Model 4 is a sensitivity analysis further adjusting Model 2 for selected markers of kidney and liver disease (creatinine, urinary specific gravity, blood urea nitrogen, alkaline phosphatase and uric acid); Model 5 is a sensitivity analysis further adjusting Model 2 for selected inflammatory factors (25-hydroxyvitamin D, serum albumin, eosinophils as % of total white blood cells); Model 6 is a sensitivity analysis further adjusting Model 2 for other lifestyle and health-related covariates (current drug use, self-rated health).

[c] P<0.10 for null hypothesis that exposure×race 2-way interaction term is =0 in the unstratified model with exposure and race included as main effects.

Table S7. Tracking high and Tracking low NfL exposures vs. Left/Right hippocampal volumes and WMLV, overall and by sex

	Tracking high NfL exposure					
	Model 1	Model 2	Model 3	Model 4	Model 5	Model 6
	Overall (n=179)					
Hippocampus, Left	**-137.94 ±50.51** **P=0.007**	**-134.84±52.12** **P=0.011**	**-139.99±52.56** **P=0.009**	**-135.47±53.97** **P=0.013**	**-130.64±54.23** **P=0.017**	**-136.16±52.68** **P=0.011**
Hippocampus, Right	**-134.12 ± 52.26** **P=0.011**	**-130.12±53.93** **P=0.017**	**-136.70±54.05** **P=0.012**	**-140.09±55.42** **P=0.012**	**-120.53±55.81** **P=0.032**	**-131.11±54.40** **P=0.017**
Lesion volume, Log_e transformed	+1.01±0.67 P=0.13	+1.13±0.69 P=0.10	+1.10±0.70 P=0.12	+1.18±0.71 P=0.098	+1.16 ± 0.71 P=0.11	+1.06±0.69 P=0.13
	Males (n=80)					
Hippocampus, Left	**-194.31±78.53** **P=0.016**	**-188.04 ±80.24** **P=0.022**	**-198.11±81.67** **P=0.018**	**-209.90± 90.55** **P=0.024**	**-207.88± 85.62** **P=0.018**	-143.60± 80.96 P=0.081
Hippocampus, Right	**-191.19± 80.71** **P=0.020**	**-175.27±81.80** **P=0.036**	**-195.03±81.85** **P=0.020**	**-230.25±89.66** **P=0.013**	**-191.28±86.01** **P=0.030**	-139.94± 83.30 P=0.098
Lesion volume, Log_e transformed	+1.32 ± 0.76 P=0.087	+1.26±0.78 P=0.11	+1.29±0.80 P=0.11	+1.77±0.85 P=0.042	+1.18±0.82 P=0.15	+1.16±0.81 P=0.16
	Females (n=99)					
Hippocampus, Left	-45.22± 64.86 P=0.49	-39.89 ± 67.57 P=0.56	-47.73±67.12 P=0.48	-29.54± 71.32 P=0.68	-21.03±70.02 P=0.77	-36.94± 66.36 P=0.58
Hippocampus, Right	-45.06±69.71 P=0.52	-46.81± 72.66 P=0.52	-51.61±73.14 P=0.48	-47.09±77.66 P=0.55	-27.25±74.99 P=0.72	-44.59±71.58 P=0.54
Lesion volume, Log_e transformed	+0.67±1.09 P=0.54	+1.05± 1.13 P=0.35	+1.03± 1.14 P=0.37	+1.05±1.20 P=0.38	+1.21± 1.18 P=0.31	+1.06 ±1.14 P=0.35

	Tracking low NfL exposure					
	Model 1	Model 2	Model 3	Model 4	Model 5	Model 6
	Overall (n=179)					
Hippocampus, Left	-14.25± 50.40 P=0.91	-19.64±50.77 P=0.70	-18.15±50.99 P=0.72	-20.92±52.54 P=0.69	-25.96±51.66 P=0.62	-20.04± 51.06 P=0.70
Hippocampus, Right	21.41± 52.01 [c] P=0.68	16.20±52.41 [c] P=0.76	+18.74 ±52.34 [c] P=0.72	+28.54 ±53.91 [c] P=0.60	+5.48± 53.53 [c] P=0.92	+15.85±52.61 [c] P=0.76
Lesion volume, Log_e transformed	-1.20±0.65 [c] P=0.066	-1.25±0.66 [c] P=0.059	-1.23±0.66 [c] P=0.063	-1.22 ±0.68 [c] P=0.074	-1.25±0.67 [c] P=0.064	-1.21± 0.66 [c] P=0.068
	Males (n=80)					
Hippocampus, Left	62.36±81.39 P=0.45	70.01±81.89 P=0.40	77.22± 82.55 P=0.35	66.30 ±88.03 P=0.45	85.21±85.52 P=0.32	57.80±79.26 P=0.47
Hippocampus, Right	137.71±82.14 P=0.10	151.44± 81.58 P=0.068	**164.39± 80.82** **P=0.046**	+164.58±85.92 P=0.060	+153.95±85.24 P=0.075	140.09±79.96 P=0.084
Lesion volume, Log_e transformed	-0.390±0.773 P=0.62	-0.448±0.779 P=0.57	-0.472±0.792 P=0.55	-0.626±0.818 P=0.45	-0.300±0.812 P=0.71	-0.407± 0.787 P=0.61
	Females (n=99)					
Hippocampus, Left	-92.34±59.78 P=0.13	-104.87±61.59 P=0.092	-92.83±61.79 P=0.14	-106.55± 65.21 P=0.11	-120.66±62.09 P=0.055	-89.18± 60.43 P=0.14
Hippocampus, Right	-86.723 64.42658± P=0.18	-93.14±66.59 P=0.17	-86.37±67.55 P=0.20	-95.72± 71.28 P=0.18	-112.81±67.06 P=0.096	-76.80±65.53 P=0.24
Lesion volume, Log_e transformed	-1.82 ±1.00 P=0.073	**-2.20 ±1.02** **P=0.035**	**-2.19 ±1.04** **P=0.039**	-1.90 ±1.09 P=0.086	**-2.33±1.05** **P=0.029**	-2.04 ±1.03 P=0.050

Abbreviations: Age_{v1}=age measured at HANDLS visit 1 (2004-2009); HANDLS=Healthy Aging in Neighborhoods of Diversity Across the Life Span; HANDLS-SCAN=Brain magnetic resonance imaging scan ancillary study of HANDLS; NfL=Neurofilament Light; SE=Standard Error; sMRI=Structural Magnetic Resonance Imaging; v_1=visit 1 of HANDLS (2004-2009); v2=visit 2 of HANDLS (2009-2013); v_{scan}=HANDLS-SCAN visit (2011-2015).

[a] Values are adjusted linear regression coefficients β with associated SE. (N) is the sample size in each analysis. Volumes are expressed in mm^3.

[b] Model 1 adjusted for Age_{v1}, sex, poverty status and length of follow-up between v_1 and v_{scan} and intracranial volume (ICV). Model 2 is Model 1 further adjusted for BMI. Model 3 is a sensitivity analysis further adjusting Model 2 for Diabetes and serum glucose levels; Model 4 is a sensitivity analysis further adjusting Model 2 for selected markers of kidney and liver disease (creatinine, urinary specific gravity, blood urea nitrogen, alkaline phosphatase and uric acid); Model 5 is a sensitivity analysis further adjusting Model 2 for selected inflammatory factors (25-hydroxyvitamin D, serum albumin, eosinophils as % of total white blood cells); Model 6 is a sensitivity analysis further adjusting Model 2 for other lifestyle and health-related covariates (current drug use, self-rated health).

[c] $P<0.10$ for null hypothesis that exposure×race 2-way interaction term is =0 in the unstratified model with exposure and race included as main effects.

Table S8. Ranking of top ROI-specific WMLV associated with NfL at v1, overall, with p<0.05: cubic root transformed WMLV

OUTCOME	idnum	EXPOSURE	Effect size	stderr	dof	t	p
zLPLIC_rightw	20	zLnNFLw1	0.383136	0.089379	171	4.286642	3.02E-05
zLfrontal_lobe_WM_right_wml	9	zLnNFLw1	0.264219	0.086229	171	3.064167	0.002537
zLfrontal_lobe_WM_left_wml	10	zLnNFLw1	0.238184	0.086363	171	2.75795	0.006449
zLRight_Lateral_Ventricle_wml	5	zLnNFLw1	0.242187	0.090636	171	2.6721	0.008267
zLLeft_Lateral_Ventricle_wml	6	zLnNFLw1	0.232254	0.090852	171	2.556383	0.011447
zLparietal_lobe_WM_right_wml	13	zLnNFLw1	0.22816	0.090593	171	2.518516	0.012703
zLRight_Caudate_wml	1	zLnNFLw1	0.223711	0.092048	171	2.430366	0.016117
zLcorpus_callosum_wml	22	zLnNFLw1	0.206543	0.092932	171	2.222516	0.02756
zLALIC_rightw	18	zLnNFLw1	0.193063	0.091697	171	2.105436	0.036714

[a] Note than only 24 ROIs were included in analysis C', given that all others were null or with <5% non-zero volume.